Some implications of a small bag radius

John A. Parmentola
University of Pittsburgh, Department of Physics and Astronomy, Pittsburgh, Pennsylvania 15260*
and Argonne National Laboratory, Physics Division, Argonne, Illinois 60439
(Received 8 December 1983)

We consider the possibility that the bag radius of the nucleon is of the order of the proton Compton wavelength. We explore this possibility for the cloudy-bag-model Hamiltonian when the interaction between the intrinsic isobar source and the pion field is turned off. Because of the large pion-nucleon coupling for a small bag radius, we apply the strong-coupling approximation to this model. Unlike other models of the nucleon with a small bag radius, our approach emphasizes the quantum-mechanical behavior of the infinitely many degrees of freedom of the pion field in the dressed nucleon wave function. Considerable attention is given to the approximate analytic solution of the strong-coupling part of the cloudy-bag-model Hamiltonian, which is a collective Hamiltonian involving nine coupled quantum-mechanical oscillators. An important feature of the model is the existence of collective excitations of the dressed nucleon which are rotational and vibrational excitations in spin and isospin space. The lowest-lying collective state is a spin and isospin rotational excitation which is identified with the Δ, while the N^* is a vibrational excitation. The approximate analytic expressions for the low-lying baryon wave functions facilitate the actual calculation of some static properties of the baryons such as masses, magnetic moments, charge radii, etc. We find for a bag radius $R=0.32$ fm that the average number of pions in the dressed nucleon state is roughly 6. Furthermore, the overall agreement between the model and experiment is roughly 30%; however, the charge radius of the proton is too small. Some speculative ideas for improving the model are discussed.

I. INTRODUCTION

Over the past few years, chiral bag models[1-5] have been a testing ground for improved models of the nucleon which incorporate quark, gluon, and pion degrees of freedom. The models presumably simulate at short distances the perturbative behavior of quantum chromodynamics, and at intermediate and large distances features of pion dynamics such as pion exchange, which is important for a proper description of nuclear-physics phenomena. While the pion is known to play an important role in the nucleon-nucleon force,[6] its role qualitatively and quantitatively in nucleon structure is unclear at present. Consequently, there are several models which attribute more or less dynamical significance to the pion in nucleon structure.

At one extreme, the original version of the MIT bag model[7] neglects explicit pion contributions to baryon spectroscopy. While the model does reasonably well phenomenologically, there are conceptual and practical problems in connecting this picture with the conventional approach to nuclear physics. The nucleon and pion have large bag radii in this model, say 1 fm, so that for a description of nuclear systems the individual nucleon and pion bags melt and the nucleus is an interacting system of quarks, gluons, and quark-antiquark pairs. Presumably, the single-particle nature of nuclear systems is a consequence of the strong color-singlet clustering of quarks within the nucleus. However, an important feature of this picture is the large number of explicit degrees of freedom and hadronic channels which are dynamically involved. In contrast, the conventional approach starts from the nonrelativistic Schrödinger equation in which the nucleon degrees of freedom are explicit and the interactions are described by two- and three-body potentials. The reasonable success of this approach[8] indicates that a model description of nuclear systems based upon quark and gluon degrees of freedom should involve a smooth connection with the conventional approach to nuclear physics. A way of incorporating this feature is to suppress the quark and gluon degrees of freedom by shrinking the bag size. This choice attributes more dynamic significance to the meson degrees of freedom for a description of the long- and intermediate-range part of the nucleon-nucleon force and for a quantitative understanding of nucleon structure.

At an intermediate level, the cloudy bag model[2] (CBM) assumes that the bag size is smaller than in the conventional MIT model, say $0.8<R<1.0$ fm, and that the pion coupling to quarks can be approximately described by a local pion field. It is unclear at a quantitative level when a local-field approximation is valid, but presumably if the low-momentum components of the pion degrees of freedom couple to the quark core of the nucleon, the internal structure of the pion can be neglected. The role of the pion in this model can be understood by considering the dressed nucleon wave function. For sufficiently large bag sizes, the strength of the meson-baryon interaction is weak, and truncation at the one-pion level in perturbation theory is valid for the nucleon self-energy and wave function. The lowest-order approximation to the nucleon state is a quark-shell-model state or bare nucleon state, and the

small corrections correspond to a bare nucleon plus a pion and a bare Δ plus a pion. These small corrections change both the quantitative and qualitative description of the proton and neutron magnetic moments. For example, in the conventional MIT bag model,[7] the ratio of the proton and neutron magnetic moments is fixed by group properties. However, their magnitudes change with the bag size. In the CBM, both the ratio and magnitudes of the magnetic moments change with the bag size. Furthermore, as the bag radius decreases, the magnetic-moment contribution from the quark core decreases and the pion contribution increases.

While the CBM model has had reasonable success phenomenologically, the validity of perturbation theory for bag sizes such that $R \leq 0.9$ fm has been recently questioned.[9]

At another extreme, the little-bag model[3] (LBM) developed by Brown and collaborators, assumes that the bag size is of the order of the proton Compton wavelength. This choice has the desirable feature of a smooth connection with conventional nuclear physics and treats the quark core of the nucleon and the pion both as small systems. According to Brown and collaborators,[3] a classical-field approximation to pion dynamics for chiral bag models is valid for a small bag radius. In their treatment, the lowest-order approximation to the nucleon wave function does not depend upon the infinitely many quantum-mechanical degrees of freedom of the pion field. However, in reality one wants to approximately solve the Schrödinger equation. And if a classical approximation to the pion-field energy of the system makes sense, then the behavior of the wave function should be such that the quantum pion field is well localized about the classical field. For example, the wave function should depend on the quantum pion field in such a way that the field fluctuates in a narrow Gaussian manner about the classical field. However, the wave functions of Brown and collaborators do not exhibit such behavior and therefore do not satisfy requirements one would expect for a system whose pion-field energy is approximately classical.

Unlike Brown and collaborators, we have found[10] for small bag sizes or strong coupling that the dressed nucleon wave function must depend on the infinitely many degrees of freedom of the meson field. In fact, the classical approximation is inadequate for a quantitative discussion of static-source meson field theories, such as the CBM and LBM, when the bag radius is small. It is essential to employ a nonperturbative quantum-mechanical computational scheme. As we have pointed out,[10] for strong coupling the average number of mesons which dress the bare nucleon can be large, and the bare-Δ-plus-meson-cloud component in the dressed nucleon state can be substantial. Furthermore, the meson cloud can be collectively excited so that excitations of the dressed nucleon exist. These features reflect the important role the meson degrees of freedom play when the bag radius or source size is small.

The basic idea of the strong-coupling approximation is to choose a basis expansion for the pion field such that the full Hamiltonian separates into a strong-coupling part which is treated precisely and a weak-coupling part which is treated perturbatively. While the essential idea behind the strong-coupling approximation is not new,[11–13] we have been able to treat the unperturbed Hamiltonian quantum mechanically for strong coupling and show quantitatively that the perturbations from the weak-coupling part are in fact small. Furthermore, we have been able to solve the meson-nucleon scattering problem[10] by employing the reaction theory of Feshbach.

In this paper, we extend the application of the strong-coupling approximation to the CBM Hamiltonian[2] when the interaction between the intrinsic isobar source and the pion field is turned off. We do not present precise numerical consequences; however, we discuss results which can be verified semiquantitatively. This has an advantage; namely, we can obtain analytic expressions for strong-coupling wave functions and energies from the model Hamiltonian. In addition, we outline a systematic method for correcting the strong-coupling approximation to wave functions and energies and we analyze qualitatively the effects produced by the small perturbations. Finally, we discuss the consequences of the strong-coupling wave functions and energies by calculating some static properties of the low-lying baryons.

The plan of this paper is as follows. In Sec. II, we define the Hamiltonian and briefly discuss the strong-coupling approximation. In Sec. III, we discuss the approximate treatment of the strong-coupling part of the Hamiltonian and we verify our results semiquantitatively. In Sec. IV, we outline a systematic method for correcting the strong-coupling approximation, and we discuss qualitatively the effects produced by the small perturbations. In Sec. V, we present results for some static properties of the low-lying baryons. In Sec. VI, we present our conclusions and a discussion of future work on improving the model.

II. THE HAMILTONIAN AND THE STRONG-COUPLING APPROXIMATION

Since the strong-coupling approximation has been described elsewhere,[10] we will be brief in setting up the problem. The Hamiltonian of interest is of the form

$$H = M_0 + \tfrac{1}{2}\sum_{\alpha}\int d^3\vec{r}\,[\pi_\alpha^2(\vec{r}) + \phi_\alpha(\vec{r})(-\nabla^2 + m_\pi^2)\phi_\alpha(\vec{r})] - g^{(0)}\sum_{\alpha i}\sigma_i\tau_\alpha\int d^3r\, U(r)\partial_i\phi_\alpha(\vec{r}) \,, \tag{2.1}$$

where M_0 is the bare mass,

$$g^{(0)} = \sqrt{4\pi} f_{NN\pi}^{(0)}/m_\pi$$

with $f_{NN\pi}^{(0)}$ the bare pion-nucleon coupling constant, the σ_i and τ_α are the usual Pauli spin and isospin matrices, m_π is the pion mass, and U is the source function given by

$$U(r) = \frac{\theta(R-r)}{V} \,, \tag{2.2}$$

where $V = 4\pi R^3/3$. The fields obey the usual commuta-

tion rules given by

$$[\pi_\alpha(\vec{r}),\phi_\beta(\vec{r}')]=-i\delta_{\alpha\beta}\delta^3(\vec{r}-\vec{r}') \ . \tag{2.3}$$

Note that the model has three free parameters, M_0, $f^{(0)}_{NN\pi}$ (see Ref. 14), and the bag radius R. In the discussion to follow, the model Hamiltonian in Eq. (2.1) and the source function in Eq. (2.2) correspond to CBM[2] when the interaction between the intrinsic isobar source and the pion field is turned off. In terms of CBM, the quark states are restricted to the bare bag proton and neutron subspace. This implies that the underlying currents, say, the electromagnetic currents, contain quark and pion contributions. We will make use of this fact in Sec. V of this paper.

It is important to note that the Hamiltonian in Eq. (2.1) is invariant under $SU(2)_J \otimes SU(2)_I$ rotations, where the group factors describe spatial rotations with total angular momentum given by

$$\vec{J}=\sum_\alpha \int d^3r\, \phi_\alpha(\vec{r})(\vec{r}\times\vec{\nabla})\pi_\alpha(\vec{r})+\frac{\vec{\sigma}}{2} \ , \tag{2.4}$$

and isospin rotations with total isospin given by

$$\vec{I}=\int d^3r\, \vec{\phi}(\vec{r})\times\vec{\pi}(\vec{r})+\frac{\vec{\tau}}{2} \ . \tag{2.5}$$

These operators will become important when we construct approximate eigenfunctions of the Hamiltonian in Sec. III.

An essential feature of the model Hamiltonian in Eq. (2.1) is the dependence of the interaction energy on the bag size, namely, as the bag size decreases the interaction energy increases so that the coupling is strong. The basic idea of the strong-coupling approximation[11–13] is to extract the largest part of the interaction energy by choosing a basis expansion for the pion field such that the full Hamiltonian separates into a strong-coupling part which is treated precisely and a weak-coupling part which is treated perturbatively. This is accomplished by decomposing the field and its canonical momentum into two orthogonal parts, namely,

$$\phi_\alpha(\vec{r})=\sum_i \partial_i F(r) q_{\alpha i}+\phi'_\alpha(\vec{r}) \tag{2.6}$$

and

$$\pi_\alpha(\vec{r})=\sum_i \partial_i F(r) p_{\alpha i}+\pi'_\alpha(\vec{r}) \ , \tag{2.7}$$

where the basic functions $\partial_i F(r)$ are normalizable functions such that

$$\int d^3r\, \partial_i F(r)\partial_j F(r)=\delta_{ij} \ , \tag{2.8}$$

and the fields $\phi'_\alpha(\vec{r})$ and $\pi'_\alpha(\vec{r})$ obey constraint conditions, namely,

$$\int d^3r\, \phi'_\alpha(\vec{r})\partial_i F(r)=0 \ , \tag{2.9}$$

and

$$\int d^3r\, \pi'_\alpha(\vec{r})\partial_i F(r)=0 \ . \tag{2.10}$$

It is straightforward to show that the $p_{\alpha i}$ and $q_{\alpha i}$ variables in Eqs. (2.6) and (2.7) are canonical, so that

$$[p_{\alpha i},q_{\beta j}]=-i\delta_{\alpha\beta}\delta_{ij} \ , \tag{2.11}$$

and $\pi'_\alpha(\vec{r})$ and $\phi'_\alpha(\vec{r})$ satisfy nonlocal commutation rules given by

$$[\pi'_\alpha(\vec{r}),\phi'_\beta(\vec{r}')]=-i\delta_{\alpha\beta}\left[\delta^3(\vec{r}-\vec{r}')-\sum_i \partial_i F(r)\partial_i F(r')\right] . \tag{2.12}$$

Some comments are in order regarding the expansion in Eq. (2.6). As a consequence of the derivative coupling in Eq. (2.1), only the p-wave components of the pion field $\phi_\alpha(\vec{r})$ participate in the interactions. The first term in Eq. (2.6) reflects the importance of the p-wave component since $\partial_i F(r)$ is proportional to a spatial unit vector. It is important to note that the field $\phi_\alpha(\vec{r})$ by definition intertwines the isospin degrees of freedom denoted by α and the angular momentum degrees of freedom which arise from the dependence of the field on $\vec{r}$. This statement means that for a given functional form and a fixed point in space the $\phi_\alpha(\vec{r})$ specify a vector in isospin space. If we perform a spatial rotation on $\vec{r}$, then the new field specifies a different isovector. This feature is manifested in the dependence of the nine quantum-mechanical variables $q_{\alpha i}$ on the isospin and spin degrees of freedom. As we shall see later, these variables will play the role of oscillator variables in the strong-coupling part of the Hamiltonian.

The arguments which motivate the choice of basis functions $\partial_i F(r)$ have been presented elsewhere[10] for the case of a SU(2)-symmetric static-source model. Roughly speaking, the basis functions $\partial_i F(r)$ are chosen such that they have a large overlap with the source function $U(r)$, given by Eq. (2.2), while the basis functions for the field $\phi'_\alpha(\vec{r})$ in Eq. (2.6) are chosen to have a small overlap with the source function.

The $\partial_i F(r)$ are proportional to the derivative of the field produced by the source so that

$$\partial_i F(r)=N\,\partial_i \hat{U}(r) \ , \tag{2.13}$$

where the field $U(r)$ is determined by

$$(-\nabla^2+m_\pi{}^2)\hat{U}(r)=U(r)=\frac{\theta(R-r)}{V} \ , \tag{2.14}$$

and N is a normalization constant fixed by Eq. (2.8). The analytic solution to Eq. (2.14) is given by

$$\hat{U}(r)=\frac{3m_\pi}{4\pi y^3}\left[[1-i_0(x)(1+y)e^{-y}]\theta(y-x)+\frac{y}{x}e^{-x}[\cosh y-i_0(y)]\theta(x-y)\right] , \tag{2.15}$$

where $x=m_\pi r$ and $y=m_\pi R$. This completes the determination of the basis functions $\partial_i F(r)$. The remaining basis functions for the weak-coupling part of the field $\phi'_\alpha(\vec{r})$, will be discussed in Sec. III B.

Upon substituting the expansions in Eqs. (2.6) and (2.7) into the Hamiltonian in Eq. (2.1), we obtain

$$H=H_c+H'+\tilde{H} \ , \tag{2.16}$$

where H_c is the collective Hamiltonian defined by

$$H_c=\tfrac{1}{2}\sum_{\alpha i}[p_{\alpha i}{}^2+\Omega^2 q_{\alpha i}{}^2+2g^{(0)}\lambda\sigma_i\tau_\alpha q_{\alpha i}]\ , \tag{2.17}$$

where the collective frequency squared Ω^2 is defined by

$$\Omega^2=\tfrac{1}{3}\sum_i\int d^3r\,\partial_i F(r)(-\nabla^2+m_\pi{}^2)\partial_i F(r) \tag{2.18}$$

and the overlap λ is defined by

$$\lambda=-\tfrac{1}{3}\sum_i\int d^3r\,U(r)\partial_i{}^2F(r)\ . \tag{2.19}$$

H' is the meson Hamiltonian defined by

$$H'=\tfrac{1}{2}\sum_\alpha\int d^3r[\pi'_\alpha{}^2(\vec{r})+\phi'_\alpha(\vec{r})(-\nabla^2+m_\pi{}^2)\phi'_\alpha(\vec{r})]\ , \tag{2.20}$$

where $\phi'_\alpha(\vec{r})$ and $\pi'_\alpha(\vec{r})$ must satisfy the constraint conditions in Eqs. (2.9) and (2.10), while the perturbation $\tilde{H}$ is given by

$$\tilde{H}=\sum_{\alpha i}\int d^3r\,\partial_i F(r)(-\nabla^2+m_\pi{}^2)\phi'_\alpha(\vec{r})q_{\alpha i} -g^{(0)}\sum_{\alpha i}\sigma_i\tau_\alpha\int d^3r\,U(r)\partial_i\phi'_\alpha(\vec{r})\ . \tag{2.21}$$

The unperturbed Hamiltonian $H^{(0)}$ is the sum of the bare mass M_0, the collective Hamiltonian H_c, and the meson Hamiltonian H', given by

$$H^{(0)}=M_0+H_c+H'\ . \tag{2.22}$$

Substituting Eqs. (2.6) and (2.7) into Eqs. (2.4) and (2.5) we obtain for the total angular momentum,

$$\vec{J}=\vec{L}+\vec{L}'+\frac{\vec{\sigma}}{2}\ , \tag{2.23}$$

where

$$L_i=\epsilon_{ijk}\sum_\alpha q_{\alpha j}p_{\alpha k} \tag{2.24}$$

with

$$\vec{L}'=\sum_\alpha\int d^3r\,\phi'_\alpha(\vec{r})(\vec{r}\times\vec{\nabla})\pi'_\alpha(\vec{r})\ , \tag{2.25}$$

and the total isospin

$$\vec{I}=\vec{T}+\vec{T}'+\frac{\vec{\tau}}{2}\ , \tag{2.26}$$

where

$$T_\alpha=\epsilon_{\alpha\beta\gamma}\sum_i q_{\beta i}p_{\gamma i} \tag{2.27}$$

with

$$\vec{T}'=\int d^3r\,\vec{\phi}'(\vec{r})\times\vec{\pi}'(\vec{r})\ . \tag{2.28}$$

Computationally, the goal is to treat the unperturbed Hamiltonian in Eq. (2.22) precisely, and obtain an infinite set of stationary states of $H^{(0)}$. The ground state of this set, the dressed nucleon state, is a reasonable approximation to the exact state provided the perturbation $\tilde{H}$ in Eq. (2.21) induces small admixtures of the unperturbed excited states into the ground state. Mathematically, this can be expressed in terms of the exact wave-function normalization given by

$$\langle\Phi_0\,|\,\Phi_0\rangle=1+\delta(\tilde{H})\ , \tag{2.29}$$

where $|\,\Phi_0\rangle$ is the exact ground state and $\delta(\tilde{H})$ is the change in the wave-function normalization due to the perturbation. In order to assess the sensibility of the computational scheme, we require that the change in the wave-function normalization, δ, decreases as the coupling constant $g^{(0)}$ increases or the bag size decreases. This condition implies that the lowest-order approximation to the exact dressed nucleon wave function is good.

While the computations associated with the evaluation of Eq. (2.29) have been carried out in a SU(2)-symmetric static-source model,[10] we will not present a detailed numerical analysis here. This will be presented in a forthcoming publication. Instead, we discuss an approximate treatment of the unperturbed Hamiltonian in Eq. (2.22) when the coupling is strong, and argue qualitatively that the perturbations produced by $\tilde{H}$ are small. There are many papers that discuss approximation methods for the energy spectrum of the collective Hamiltonian in Eq. (2.17). Essentially, there have been three approaches to H_c. The first employs a variational principle which is based upon trial wave functions constructed from coherent states.[9,15] Another approach attempts to diagonalize the Hamiltonian in a subspace of states which are characterized by a definite number of mesons.[16] Finally, there is the semiclassical approach[12] which approximates the energy spectrum of the collective Hamiltonian by the minimum value of the potential energy, and includes some quantum-mechanical effects through the rotational energy of the system of oscillators. For strong coupling, the variational and diagonalization approaches are difficult to carry out.[15] This difficulty can be traced to the dependence of the number of basis states on the coupling strength, namely, as the coupling strength increases the number of basis states increases. On the other hand, while the semiclassical approximation is easy to implement, it is unclear how to calculate corrections and verify the approximation.

In the next section, we discuss a strong-coupling-approximation method for the collective Hamiltonian which does not have the above limitations. We obtain approximate analytic expressions for wave functions and energies which can be verified semiquantitatively. It is important to note that our method of approximation of the full Hamiltonian in Eq. (2.1) is not the single-mode approximation,[9,15] since we approximately diagonalize the unperturbed Hamiltonian in Eq. (2.22). This implies that our lowest-order wave functions depend on the infinitely many degrees of freedom of the pion field.

III. THE UNPERTURBED HAMILTONIAN

A. The collective Hamiltonian

For small bag sizes or strong coupling, we expect that the interaction-energy operator $\sum_{\alpha i}\sigma_i\tau_\alpha q_{\alpha i}$ in Eq. (2.17)

will be the dominant term in the collective Hamiltonian. This is a consequence of the dependence of the overlap λ defined by Eq. (2.19) on the bag size R. A straightforward computation for $R \ll 1/m_\pi$ gives

$$\lambda \cong \left[\frac{5}{8\pi}\right]^{1/2}\left[\frac{1}{R}\right]^{5/2} . \tag{3.1}$$

This implies that there are modes of the pion field which contribute a large interaction energy to the collective Hamiltonian. Furthermore, the modes have high momenta[10] which are of the order $1/R$. The average energy of these modes is the collective frequency Ω defined by Eq. (2.18). A straightforward computation for $R \ll 1/m_\pi$ gives

$$\Omega \cong \left[\frac{5}{2}\right]^{1/2}\frac{1}{R} . \tag{3.2}$$

Since the overlap λ in Eq. (3.1) is large[17] for $R \ll 1/m_\pi$, we proceed as in the Paschen-Back effect by choosing a basis for the collective Hamiltonian which diagonalizes the interaction-energy operator in Eq. (2.17). The relevant eigenvalue equation is given by

$$\sum_{\alpha i} \sigma_i \tau_\alpha q_{\alpha i} \mid \Lambda,\eta\rangle = \eta \mid \Lambda,\eta\rangle , \tag{3.3}$$

where Λ represents a set of quantum numbers to be specified later and η are the eigenvalues. The operator $\sum_{\alpha i}\sigma_i\tau_\alpha q_{\alpha i}$ is a 4×4 matrix which is a continuous function of the $q_{\alpha i}$, hence, there are four continuous eigenvalues. A convenient choice of variables for representing these eigenvalues has been discussed in a pioneering paper by Pauli and Dancoff.[12] They showed that the nine Cartesian variables $q_{\alpha i}$ can be expressed in terms of three Euler angles which describe dynamical rotations of a set of body-fixed axes in ordinary three-vector space, a similar set of three Euler angles in isospace, and three radial variables. Mathematically, the change of variables is given by

$$q_{\alpha i} = \sum_{r=1}^{3} B^T_{\alpha r} Q_r A_{ri} , \tag{3.4}$$

where[12] A_{ri} is a proper orthogonal rotation matrix in ordinary three-vector space which is parametrized by three Euler angles $\{\phi,\theta,\psi\}$, $B_{r\alpha}$ is a similar matrix in isospace parametrized by three Euler angles $\{\Phi,\Theta,\Psi\}$, and the Q_r are three radial variables. Roughly speaking, Eq. (3.4) expresses the intertwining of two three-vector spaces labeled by α and i through the body-fixed axes labeled by r, where the amount of intertwining depends on the values of the radial variables Q_r. An analog to Eq. (3.4) is the relation between the Cartesian variables x, y, and z, and spherical polar coordinates. The spherical polar system describes a dynamical rotation of a set of "body-fixed" axes, where the body-fixed z axis lies along the radial direction.

Since the problem of determining the eigenvalues of Eq. (3.4) has been discussed by Pauli and Dancoff, we sketch their results. Under an appropriate unitary rotation of the spin and isospin matrices, Eq. (3.3) becomes

$$\sum_r \sigma_r\tau_r Q_r u \mid \Lambda,\eta\rangle = \eta u \mid \Lambda,\eta\rangle , \tag{3.5}$$

where u is the unitary rotation matrix given by

$$u = u_\sigma u_\tau \tag{3.6}$$

with

$$u_\sigma = \begin{bmatrix} e^{-(i/2)(\phi+\psi)}\cos\frac{\theta}{2} & e^{-(i/2)(\phi-\psi)}\sin\frac{\theta}{2} \\ e^{(i/2)(\phi-\psi)}\sin\frac{\theta}{2} & e^{(i/2)(\phi+\psi)}\cos\frac{\theta}{2} \end{bmatrix} , \tag{3.7}$$

and u_τ is obtained from u_σ by replacing $\phi\to\Phi$, $\psi\to\Psi$, and $\theta\to\Theta$. Since $[\sigma_r\tau_r,\sigma_s\tau_s]=0$, $(\sigma_r\tau_r)^2=1$, and $\sigma_n\tau_n\sigma_s\tau_s\sigma_t\tau_t=-1$, it follows that

$$\begin{aligned} \eta_1 &= -Q_1-Q_2-Q_3 , \\ \eta_2 &= -Q_1+Q_2+Q_3 , \\ \eta_3 &= Q_1-Q_2+Q_3 , \\ \eta_4 &= Q_1+Q_2-Q_3 , \end{aligned} \tag{3.8}$$

The resemblance of the operator $\sum_r \sigma_r\tau_r Q_r$ when $Q_1=Q_2=Q_3=1$ to the operator $\vec{\sigma}_1\cdot\vec{\sigma}_2$ involving two spin-$\frac{1}{2}$ particles is useful. The eigenvalues of $\vec{\sigma}_1\cdot\vec{\sigma}_2$ are -3 and 1 which correspond to singlet and triplet states, respectively. For Eq. (3.8) the singlet eigenvalue is η_1 and the triplet eigenvalues are η_2, η_3, and η_4. The singlet state is such that 3-components of the bare nucleon spin and isospin are oppositely oriented. This observation will become useful when we discuss baryon magnetic moments in Sec. V.

There are two important problems which must be discussed before we construct the eigenfunctions of the interaction operator in Eq. (3.3) and the approximate eigenfunctions of the collective Hamiltonian in Eq. (2.17). The first involves the determination of the measure associated with the change of variables defined by Eq. (3.4). The second involves the parameter space of the six Euler angles and the three radial variables.

The first problem has been partially discussed by Pais and Serber.[18] We express their results in terms of the equivalence of volume integrals such that

$$\begin{aligned} &\int_{-\infty}^{\infty}\prod_{\alpha i} dq_{\alpha i} \\ &\quad = \int d\Omega_L \int_{\{P\}} d\Omega_T \int dQ_1 dQ_2 dQ_3 M(Q_1,Q_2,Q_3) , \end{aligned} \tag{3.9}$$

where

$$\begin{aligned} d\Omega_L &= \sin\theta\, d\theta\, d\phi\, d\psi , \\ d\Omega_T &= \sin\Theta\, d\Theta\, d\Phi\, d\Psi , \\ M(Q_1,Q_2,Q_3) &= (Q_1^2-Q_2^2)(Q_2^2-Q_3^2)(Q_1^2-Q_3^2) , \end{aligned} \tag{3.10}$$

and $\{P\}$ is the second problem, namely, the parameter space of the new variables. A detailed discussion of the parameter space $\{P\}$ is presented in Appendix A. There we consider a simpler problem involving four Cartesian variables and we extend this analysis to the nine-variable problem of Eq. (3.4). The essential result is given by

$$\int_{-\infty}^{\infty}\prod_{\alpha i} dq_{\alpha i}=\int_0^{2\pi}d\phi\int_0^{\pi}\sin\theta\,d\theta\int_0^{2\pi}d\psi\int_0^{\pi}d\Phi\int_0^{\pi}\sin\Theta\,d\Theta\int_0^{\pi}d\Psi\int_0^{\infty}dQ_1\int_0^{Q_1}dQ_2\int_{-Q_2}^{Q_2}dQ_3 M(Q_1,Q_2,Q_3)\,. \tag{3.11}$$

Geometrically, the region of integration of the Q_r's is a tetrahedron with one boundary plane at infinity as shown in Fig. 1. Note that $M(Q_1,Q_2,Q_3)$ is positive in this region. For those who doubt the equivalence expressed by Eq. (3.11), we suggest the following test. Consider the collective Hamiltonian in Eq. (2.17) when $g^{(0)}=0$, then we have a system of nine uncoupled oscillators. The unnormalized ground-state wave function is given by

$$\Psi_0=\exp\left[-\frac{\Omega}{2}\sum_{\alpha i} q_{\alpha i}{}^2\right], \tag{3.12}$$

and upon substituting Eq. (3.4) in Eq. (3.12) we have

$$\Psi_0=\exp\left[-\frac{\Omega}{2}\sum_{r} Q_r{}^2\right]. \tag{3.13}$$

Now, it is possible but tedious to show that the norm of the wave function in Eq. (3.12) is equal to the norm of Ψ_0 in Eq. (3.13) when the appropriate measure in Eq. (3.11) is used.

Some useful insights into the interpretation of Eq. (3.11) can be obtained by considering the usual one-body problem in three-vector space. For spherical-polar coordinates, it is well known that the integration measure vanishes when the radial variable is zero. This point is a boundary point of the parameter space, and furthermore, a singular point of the one-body Schrödinger equation. Similarly, when $Q_1=Q_2$ in Eq. (3.11), we have a boundary plane of the parameter space, and we expect that this is a singular plane of the corresponding Schrödinger equation. Similar statements apply to the entire tetrahedral boundary in Fig. 1.

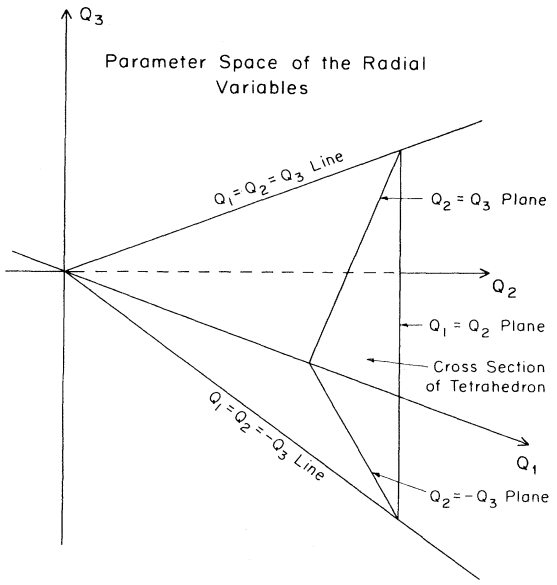

FIG. 1. A plot of the parameter space of the Q_r's which is defined by Eq. (A21). The fourth boundary plane is at infinity.

Naively, one might think that the parameter space of the Euler angles is the standard choice, however, this is not the case as indicated by Eq. (3.11).[19] This is a consequence of a set of discrete transformations defined by Eqs. (A23) and (A24) in the body-fixed frame which leave Eq. (3.4) invariant. Such transformations imply that the standard choice contains redundant regions of integration (See Appendix A).

Pais and Serber[18] have shown that the collective Hamiltonian can be expressed in terms of the radial and angular variables of Eq. (3.4) such that

$$H_c=K+H_{cb}+U\,, \tag{3.14}$$

where

$$\begin{aligned} K&=-\tfrac{1}{2}\sum_r \frac{1}{M}\frac{\partial}{\partial Q_r}M\frac{\partial}{\partial Q_r}\,,\\ H_{cb}&=\tfrac{1}{8}\sum_{rs}\frac{(\hat{L}_{rs}+\hat{T}_{rs})^2}{(Q_r-Q_s)^2}+\frac{(\hat{L}_{rs}-\hat{T}_{rs})^2}{(Q_r+Q_s)^2}\,,\\ U&=\tfrac{1}{2}\left[\Omega^2\sum_r Q_r{}^2+2g^{(0)}\lambda\sum_{\alpha i r}\sigma_i\tau_\alpha B^T_{\alpha r}Q_r A_{ri}\right], \end{aligned} \tag{3.15}$$

with $\hat{L}_{rs}$ and $\hat{T}_{rs}$ the Cartesian components of the body-fixed angular momentum and isospin operators, respectively, and M is given by Eq. (3.10). The body-fixed operators are related to the corresponding inertial quantities via a rotation, namely,

$$\begin{aligned} \hat{L}_i&=\sum_j A_{ij}L_j\,,\\ \hat{T}_\alpha&=\sum_\beta B_{\alpha\beta}T_\beta\,, \end{aligned} \tag{3.16}$$

where L_j and T_β are given by Eqs. (2.24) and (2.27), respectively. The body-fixed operators satisfy the well-known anomalous commutation relations.[18]

While the Hamiltonian in Eq. (3.14) looks formidable, the operators K, H_{cb}, and U have simple interpretations which are familiar from the one-body Schrödinger equation. For example, K in Eq. (3.15) is the radial kinetic energy, H_{cb} is a generalization of the usual centrifugal barrier, and U is the potential energy. Note that the kinetic energy and centrifugal barrier have singular points and planes. This implies that the eigenfunctions of H_c must satisfy boundary conditions at these singularities so that the energy of the system of oscillators is finite.

According to Eq. (3.3), we must specify the set of quantum numbers Λ which label the eigenstates of the interaction operator. The symmetry operators which commute with $\sum_{\alpha i}\sigma_i\tau_\alpha q_{\alpha i}$ are given by

$$J_i^c = L_i + \sigma_i/2 ,$$
$$I_\alpha^c = T_\alpha + \tau_\alpha/2 ,$$
$$\hat{J}_i = \hat{L}_i + \hat{\sigma}_i/2 , \tag{3.17}$$
$$\hat{I}_\alpha = \hat{T}_\alpha + \hat{\tau}_\alpha/2 ,$$

where $\hat{\sigma}_i$ and $\hat{\tau}_\alpha$ are related to σ_i and τ_α via rotations as in Eq. (3.16). Note that the operators J_i^c and I_α^c commute with the body-fixed operators $\hat{J}_i$ and $\hat{I}_\alpha$. This implies that the quantum numbers Λ can be chosen such that

$$|\Lambda,\eta_i\rangle = |j^c,j_z^c,\hat{j}_z;i^c,i_z^c,\hat{i}_z;\eta_i\rangle . \tag{3.18}$$

The motivation for introducing the body-fixed quantum numbers, $\hat{j}_z$ and $\hat{i}_z$ involves the centrifugal barrrier in Eq. (3.15), which depends on the body-fixed angular momentum and isospin operators. Eventually, we will take matrix elements of the centrifugal barrier with respect to the basis states in Eq. (3.18). For the evaluation of the matrix elements, we can take advantage of a version of the Wigner-Eckart theorem for body-fixed operators.

Since the collective Hamiltonian is not diagonal in the quantum numbers $\hat{j}_z$, $\hat{i}_z$, and η_i, we express the eigenfunctions of H_c as a linear combination of the basis states of Eq. (3.18) such that

$$|\Psi\rangle = \sum_{\hat{j}_z,\hat{i}_z,\eta_i} W_{\hat{j}_z\hat{i}_z\eta_i} |j^c,j_z^c,\hat{j}_z;i^c,i_z^c,\hat{i}_z;\eta_i\rangle , \tag{3.19}$$

where the W's are functions of the radial variables Q_r. The basis expansion in Eq. (3.19) spans a space which is too large for the collective Hamiltonian. This can be traced to the change of variables defined by Eq. (3.4). As we have shown in Appendix A, there are a set of discrete transformations in the body-fixed frame defined by Eqs. (A23) and (A24) which leave Eq. (3.4) invariant. In Appendix B, we show that this invariance implies a set of conditions on the radial functions W in Eq. (3.19). We implicitly include the conditions of Eqs. (B6) and (B7) by replacing $\sum$ by $\sum'$ in Eq. (3.19), so that

$$|\Psi\rangle = \sum_{\hat{j}_z,\hat{i}_z,\eta_i}{}' W_{\hat{j}_z\hat{i}_z\eta_i} |j^c,j_z^2,\hat{j}_z;i^c,i_z^c,\hat{i}_z;\eta_i\rangle . \tag{3.20}$$

In order to make further progress in understanding the energy spectrum of the collective Hamiltonian defined by Eq. (3.14), we must make approximations. We will rely on our analysis of the SU(2) static-source model[10] and draw heavily on analogies with this model.

The starting point for our analysis of the collective Hamiltonian is the potential energy U defined by Eq. (3.15). Using the basis states in Eq. (3.18), we define eigenpotentials such that

$$U|\Lambda,\eta_i\rangle = u_i|\Lambda,\eta_i\rangle \tag{3.21}$$

with the u_i given by

$$u_1 = \tfrac{1}{2}\left[\Omega^2\sum_r Q_r{}^2 - 2g^{(0)}\lambda(Q_1+Q_2+Q_3)\right] ,$$
$$u_2 = \tfrac{1}{2}\left[\Omega^2\sum_r Q_r{}^2 - 2g^{(0)}\lambda(Q_1-Q_2-Q_3)\right] ,$$
$$u_3 = \tfrac{1}{2}\left[\Omega^2\sum_r Q_r{}^2 - 2g^{(0)}\lambda(-Q_1+Q_2-Q_3)\right] , \tag{3.22}$$
$$u_4 = \tfrac{1}{2}\left[\Omega^2\sum_r Q_r{}^2 - 2g^{(0)}\lambda(-Q_1-Q_2+Q_3)\right] ,$$

which follow from Eq. (3.8). An important feature of the u_i is the fact that the potential energy minimum of u_1 is the lowest. This can be demonstrated in the usual way subject to the restriction of the parameter space of the Q_r's, namely,

$$\infty > Q_1 \geq Q_2 \geq |Q_3| \geq 0 . \tag{3.23}$$

The minimum in u_1 is located at the point given by

$$\bar{Q}_1 = \bar{Q}_2 = \bar{Q}_3 = g^{(0)}\lambda/\Omega^2 \cong g^{(0)}/(10\pi R)^{1/2} \tag{3.24}$$

with a value such that

$$\bar{u}_1 = \frac{-3g^{(0)2}\lambda^2}{2\Omega^2} \cong \frac{-3g^{(0)2}}{8\pi R^3} , \tag{3.25}$$

when $R \ll 1/m_\pi$. The potential-energy difference $u_1 - \bar{u}_i$ for $i \geq 2$ is roughly of the order of $-g^{(0)2}\lambda^2/\Omega^2$ or less. As a consequence, we refer to the η_1 states as low-lying states and the η_i states with $i \geq 2$ as high-lying states. From the large energy separation between the low-lying and high-lying states for a small bag radius, we expect that the corresponding radial wave functions W_{η_i} will be localized in different regions of the tetrahedron in Fig. 1. For example, Eq. (3.24) implies that the low-lying radial wave function W_{η_1} is localized somewhere along the line $Q_1 = Q_2 = Q_3$ in Fig. 1, while the minimum in u_2 indicates that the high-lying radial wave function W_{η_2} is localized somewhere along the Q_1 axis. Similarly, W_{η_3} and W_{η_4} are localized near the origin. Furthermore, from the harmonic-oscillator nature of u_1, we expect that the lowest-lying state will be a Gaussian in the Q_r's localized about the point defined by Eq. (3.24). Therefore, as the bag radius goes to zero the overlap between the low-lying and high-lying radial wave functions will go to zero rapidly. Hence, we can simplify the collective Hamiltonian by noting that the centrifugal barrier H_{cb} defined by Eq. (3.15) is the only operator in Eq. (3.14) which has off-diagonal matrix elements in η_i. Therefore, for a small bag radius the matrix elements of H_{cb} between the low-lying and the high-lying states will be negligible as a result of the small overlap between the radial wave functions, W_{η_1} and W_{η_i} for $i \geq 2$. Furthermore, if we perturb about the ground state in the off-diagonal elements in η_i of H_{cb}, then the corrections to the ground-state wave function will be characterized by large energy denominators and small numerators when $R \ll 1/m_\pi$. Therefore, for strong coupling or a small bag radius the low-lying spectrum

decouples from the high-lying spectrum. This feature occurs in the SU(2) static source model.

For strong coupling and a discussion of the low-lying spectrum, we can restrict the summation in Eq. (3.20) to states with $\eta_i=\eta_1$. If we specialize for the moment to low-lying states with $j^c=i^c=\frac{1}{2}$, then Eq. (3.20) is approximately given by Eq. (B8), namely,

$$|\Psi\rangle \cong W(\,|\,\tfrac{1}{2},j_z^c,\tfrac{1}{2};\tfrac{1}{2},i_z^c,-\tfrac{1}{2};\eta_1\rangle - |\,\tfrac{1}{2},j_z^c,-\tfrac{1}{2};\tfrac{1}{2},i_z^c,\tfrac{1}{2};\eta_1\rangle)\,, \tag{3.26}$$

where we have suppressed the η_1 label on W. In order to obtain an equation for W, we must calculate the matrix elements of H_{cb} with respect to the basis states in brackets in Eq. (3.26). In Appendix C, we discuss a method for explicitly constructing these states and the evaluation of the matrix elements of H_{cb}. Upon operating with the collective Hamiltonian H_c defined by Eq. (3.14) on the wave function defined by Eq. (3.26) and then taking matrix elements with respect to the basis states in brackets in Eq. (3.26), we obtain an equation for W of the form

$$\frac{1}{2}\left[\sum_r\left[-\frac{\partial^2}{\partial Q_r^{\,2}}+\Omega^2 Q_r^{\,2}-2g^{(0)}\lambda Q_r\right]-\sum_{r<s}\frac{1}{Q_r-Q_s}\left[\frac{\partial}{\partial Q_r}-\frac{\partial}{\partial Q_2}\right]-\sum_{r<s}\frac{1}{Q_r+Q_s}\left[\frac{\partial}{\partial Q_r}+\frac{\partial}{\partial Q_s}\right]+\sum_{r<s}\frac{1}{(Q_r+Q_s)^2}\right]W=EW\,, \tag{3.27}$$

where we have made use of Eqs. (3.10) and (3.15) to rewrite the kinetic energy operator and Eq. (3.22) for the eigenpotential u_1. An interesting feature of Eq. (3.27) is the absence of energy contributions from the centrifugal barrier H_{cb} which depend upon the $(\hat{L}_{rs}+\hat{T}_{rs})^2$ terms.[12,18] This is true for the lowest-energy states with $j^c=i^c$, however we will not prove this here. Furthermore, states with $j^c\neq i^c$ have contributions from both $(\hat{L}_{rs}+\hat{T}_{rs})^2$ and $(\hat{L}_{rs}-\hat{T}_{rs})^2$ terms. Since these contributions are positive, we expect that the lowest state with $j^c=i^c=\frac{1}{2}$ or $j^c=i^c=\frac{3}{2}$ will be lower in energy than states with ($j^c=\frac{1}{2}$; $i^c=\frac{3}{2}$) or ($j^c=\frac{3}{2}$; $i^c=\frac{1}{2}$).

To obtain insight into the solutions of Eq. (3.27), it is useful to refer to the parameter space of the Q_r's in Fig. 1. The singularities of the differential operator of Eq. (3.27) are located on the boundaries of the tetrahedral volume in Fig. 1. The presence of such singularities implies restrictions on the behavior of W as a function of the Q_r's at the boundaries. For example, as $Q_3\to -Q_2$, W must have the correct power-law behavior on the boundary, say, $(Q_3+Q_2)^\lambda$ for some specific λ, so that the energy contribution from the centrifugal barrier is finite. In general, the correct power-law behavior on all boundaries is difficult to incorporate in W. However, for strong coupling there is a significant simplification which is a consequence of the behavior of eigenpotential u_1 defined by Eq. (3.22). We have argued above that the minimum in u_1 implies that the low-lying radial wave function W is localized somewhere along the line $Q_1=Q_2=Q_3$. The approximate location is the point given by Eq. (3.24). As the bag radius goes to zero, this point moves further out along the line, so that the singularities at the origin $Q_1=Q_2=Q_3=0$, on the plane $Q_3=-Q_2$, and along the line $Q_3=-Q_1=-Q_2$ are far away from the region where W is largest, i.e., the effects of these singularities on the radial wave function are small. Similar behavior of the low-lying radial wave function occurs in the SU(2) static-source model, however, there is an important difference. Suppose we rewrite Eq. (3.27) such that

$$(h_0+h')W=EW\,, \tag{3.28}$$

where

$$h_0=\frac{1}{2}\left[\sum_r\left[-\frac{\partial^2}{\partial Q_r^{\,2}}+\Omega^2 Q_r^{\,2}-2g^{(0)}\lambda Q_r\right]-\sum_{r<s}\frac{1}{Q_r-Q_s}\left[\frac{\partial}{\partial Q_r}-\frac{\partial}{\partial Q_s}\right]\right] \tag{3.29}$$

and

$$h'=-\frac{1}{2}\sum_{r<s}\frac{1}{Q_r+Q_s}\left[\frac{\partial}{\partial Q_r}+\frac{\partial}{\partial Q_s}\right]+\frac{1}{2}\sum_{r<s}\frac{1}{(Q_r+Q_s)^2}\,.$$

The above argument indicates that for sufficiently strong coupling, h' can be treated as a perturbation since it is negligible in the region where W is large. However, the centrifugal-energy operator

$$h'_{cb}=\frac{1}{2}\sum_{r<s}\frac{1}{(Q_r+Q_s)^2} \tag{3.30}$$

is such that the expectation value of h'_{cb} with respect to the unperturbed eigenfunctions of h_0 diverges. This divergence is a consequence of the measure defined by Eq. (3.11) and the fact that the unperturbed radial wave function does not have the correct behavior on the distant singular boundaries where it is small. A similar problem occurs for the radial equation of a two-dimensional harmonic oscillator with a linear-coupling potential. In the latter case, an approximate solution for strong coupling is obtained by expanding the centrifugal energy about the minimum in the potential energy. So, if we naively neglect the region in the neighborhood of the distant singular boundaries, we can treat h' in Eq. (3.29) as a perturbation and obtain an approximate result for the first-order energy shift in h'. In fact, for strong coupling the derivative terms in Eq. (3.29) are entirely negligible, since the derivative of the radial wave function is approximately zero in the region where the wave function is largest and well localized. In Appendix D, we solve the eigen-

value problem for h_0 defined by Eq. (3.28). The results for the two lowest eigenvalues when $j^c=i^c=\frac{1}{2}$ are given by

$$E^{(0)}_{0(1/2)(1/2)} \cong 3\Omega + \frac{3\Omega}{16x_0{}^2} - \Omega x_0{}^2 \tag{3.31}$$

and

$$E^{(0)}_{1(1/2)(1/2)} \cong \Omega + E^{(0)}_{0(1/2)(1/2)} , \tag{3.32}$$

where the dimensionless quantity x_0 is given by Eq. (D9). The first term in Eq. (3.31) is the zero-point energy of the ground state, the second term is the centrifugal energy, and the last term is the potential energy. The excited-state energy defined by Eq. (3.32) corresponds to a vibrational excitation of the system which is Ω above the ground state.

A similar analysis can be applied to the case when $j^c=i^c=\frac{3}{2}$. An analogous equation to Eq. (3.28) is obtained; however, the centrifugal energy in Eq. (3.29) is larger by a factor of 6, so that

$$E^{(0)}_{0(3/2)(3/2)} \cong 3\Omega + \frac{9\Omega}{8x_0{}^2} - \Omega x_0{}^2 . \tag{3.33}$$

The dimensionless quantity x_0 in Eq. (D9) plays an important role in the strong-coupling approximation, since it is a measure of the displacement of the low-lying radial function from the less important singular boundaries. Summarizing the above discussion, if $x_0 \gg 1$ we expect that our strong-coupling results are a reasonable approximation to the collective Hamiltonian in Eq. (3.14). In Fig. 2 we plot x_0 as a function of the bag radius R for a physical value of the bare coupling constant $g^{(0)}$ (see Sec. V of this paper). Hence, we expect that the strong-coupling approximation is valid for bag radii such that $R \leq 0.35$ fm.

B. The meson Hamiltonian

In this section we discuss the eigenvalues and eigenvectors of H' defined by Eq. (2.20). Since a similar problem has been solved previously,[10] we will be brief. In order to obtain the eigenvalues and eigenfunctions of H', we proceed as in free-field theory by specifying a basis which diagonalizes the Klein-Gordon operator; however, this basis must be chosen orthogonal to $\partial_i F(r)$ so that the constraint conditions defined by Eqs. (2.9) and (2.10) are satisfied.

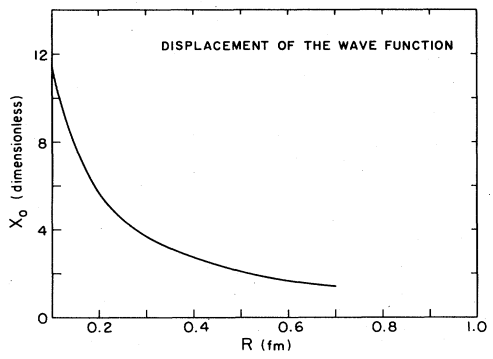

FIG. 2. A plot of x_0 defined by Eq. (D9) as a function of the bag radius R.

A convenient way of obtaining this basis is to define an operator such that

$$\hat{h} = \left[1 - \sum_i |G_i\rangle\langle G_i|\right](-\nabla^2 + m_\pi{}^2) \times \left[1 - \sum_i |G_i\rangle\langle G_i|\right] , \tag{3.34}$$

where $\langle \vec{r}\,|\,G_i\rangle = \partial_i F(r)$. Note that $\hat{h}$ is the projection of the Klein-Gordon operator onto a space orthogonal to the $\partial_i F(r)$ and $\hat{h}$ has three zero-energy bound-state solutions, namely, the $\partial_i F(r)$. It is straightforward to obtain the eigenvalues and eigenfunctions of $\hat{h}$ as we have shown.[10] The eigenfunctions describe the scattering of a pion in a background potential which depends on $\partial_i F(r)$. These scattering solutions are the expansion functions for the fields $\phi'_\alpha(\vec{r})$ and $\pi'_\alpha(\vec{r})$ which when substituted in Eq. (2.20) reduce the eigenvalue problem of H' to normal mode form. It can be shown that this implies that H' has a discrete energy eigenvalue, the pion vacuum energy, and a continuous spectrum of multipion energies. The vacuum state and the pion states are not free-field states. Furthermore, the vacuum energy is not the free-field vacuum energy, however, the pion energies have the free-field form.

The pion vacuum energy or total zero-point energy of H' is given by

$$E'_{\rm vac} = E_{\rm vac} - E_{\rm shift} , \tag{3.35}$$

where $E_{\rm vac}$ is the usual free-field vacuum energy given by

$$E_{\rm vac} = \frac{3V}{2}\int \frac{d^3k}{(2\pi)^3}\omega(k) \tag{3.36}$$

with V the volume of all space, $\omega(k)=(k^2+m_\pi{}^2)^{1/2}$, and $E_{\rm shift}$ is given by

$$E_{\rm shift} = \tfrac{3}{2}\sum_i \int d^3r\, d^3r' \partial_i F(r) f(\vec{r},\vec{r}') \partial'_i F(\vec{r}') \tag{3.37}$$

with

$$f(\vec{r},\vec{r}') = \int \frac{d^3k}{(2\pi)^3} e^{i\vec{k}\cdot(\vec{r}-\vec{r}')}\omega(k) . \tag{3.38}$$

Note that $E_{\rm shift}$ depends on the source size R through $\partial_i F(r)$, and therefore contributes to the ground-state energy of the system, while $E_{\rm vac}$ is a divergent and cutoff-dependent contribution. We will absorb $E_{\rm vac}$ into a redefinition of the bare mass M_0 appearing in Eq. (2.1).

Combining Eqs. (3.31), (3.37), and the bare mass M_0, the physical mass of the nucleon is given by

$$M_N = M_0 + E_{(0(1/2)(1/2)} - E_{\rm shift} , \tag{3.39}$$

and the dressed nucleon state is given by

$$|N\rangle = |\Psi,^{(0)}\eta_1\rangle\,|0'\rangle , \tag{3.40}$$

where $|\Psi^{(0)},\eta_1\rangle$ is given by Eq. (D26) and $|0'\rangle$ is the ground state of H'. The masses of the Δ and N^* are obtained in a similar manner, namely,

$$M_\Delta = M_0 + E^{(0)}_{0(3/2)(3/2)} - E_{\text{shift}} , \tag{3.41}$$

and

$$M_{N^*} = M + E^{(0)}_{1(1/2)(1/2)} - E_{\text{shift}} , \tag{3.42}$$

where $E^{(0)}_{0(3/2)(3/2)}$ and $E^{(0)}_{1(1/2)(1/2)}$ are given by Eqs. (3.33) and (3.32), respectively. The wave functions for the Δ and N^* are straightforward to obtain from the results of Appendices C and D.

IV. THE PERTURBATIONS

In this section, we discuss the effects produced by the perturbation Hamiltonian $\tilde{H}$ defined by Eq. (3.21). The discussion is at a qualitative level; however, we argue that the admixtures induced by $\tilde{H}$ into the nucleon ground state are small for strong coupling. The arguments follow our previous discussion of the SU(2) static source model.[10]

For convenience, we add and subtract a term in $\tilde{H}$ such that

$$\tilde{H} = N \sum_{\alpha i} \int d^3r \, \partial_i U(r) \phi'_\alpha(\vec{r}) \sum_r B^T_{\alpha r}(Q_r - \bar{Q}_r) A_{ri} - g^{(0)} \sum_{\alpha i} (e_{\alpha i} + \tau_\alpha \sigma_i) \int d^3r \, U(r) \partial_i \phi'_\alpha(\vec{r}) , \tag{4.1}$$

where the $e_{\alpha i}$ are given by

$$e_{\alpha i} = \sum_r B^T_{\alpha r} A_{ri} , \tag{4.2}$$

and the $\bar{Q}_r$'s are given by Eq. (3.24). Note that we have used the definition of $\partial_i F(r)$ in Eq. (2.13), the field equation of Eq. (2.14), and the change of variables defined by Eq. (3.4).

Since the operator $\tilde{H}$ in Eq. (4.1) is linear in $\phi'_\alpha(\vec{r})$, then matrix elements of $\tilde{H}$ between eigenstates of $H^{(0)}$ in Eq. (2.22) involve states which differ by one-pion scattering in a background potential. If we perturb in $\tilde{H}$ about the nucleon ground state of $H^{(0)}$, then $\tilde{H}$ contributes in second order.

The properties of the states defined by Eqs. (3.3) and (3.18) are important for a discussion of the effects of $\tilde{H}$ on the nucleon ground state. From Eq. (3.3) it is straightforward to show that

$$\langle \Lambda', \eta_j \mid \Lambda, \eta_i \rangle = \delta_{\Lambda'\Lambda} \delta_{\eta_j \eta_i} , \tag{4.3}$$

where the inner product is only in spinor space and does not involve an integration over Euler angles, etc. Another useful property which follows from an application of the Wigner-Eckart theorem is given by

$$\langle \Lambda', \eta_1 \mid \tau_\alpha \sigma_i \mid \Lambda, \eta_1 \rangle = - \langle \Lambda', \eta_1 \mid e_{\alpha i} \mid \Lambda, \eta_1 \rangle . \tag{4.4}$$

This is a generalization of the projection theorem[10] of the SU(2) static-source model. In Sec. III, we argued that the nucleon ground state of $H^{(0)}$ is approximately given by Eq. (3.40). From Eq. (3.40), it follows that the nucleon state is an eigenstate of the interaction-energy operator in Eq. (3.3) with eigenvalue η_1 given by Eq. (3.8). This fact and the orthogonal conditions expressed by Eq. (4.3) imply that the first term in $\tilde{H}$, i.e., the term proportional to N, induces transitions between the nucleon state and the low-lying states such as, the $N+\pi$, $\Delta+\pi$, $N^*+\pi$, etc. There are no matrix elements of the first term between the nucleon state and the high-lying states. Furthermore, Eq. (4.4) implies that the second term in $\tilde{H}$ induces transitions between the nucleon state and the high-lying states, i.e., states with η_i where $i \geq 2$. There are no matrix elements of the second term between the nucleon state and the low-lying states.

An important feature of $\tilde{H}$ is the dependence of the first term on $(Q_r - \bar{Q}_r)$. The $\bar{Q}_r$ specify the location of the minimum of the eigenpotential u_1 and the point about which the low-lying radial wave functions W fluctuate and are well localized. This implies that the radial matrix elements of $(Q_r - \bar{Q}_r)$ between the nucleon state and the low-lying states such as $N+\pi$ and $\Delta+\pi$ go to zero rapidly as the bag radius goes to zero. Furthermore, the radial matrix element of $(Q_r - \bar{Q}_r)$ between the nucleon state and the $N^*+\pi$ also goes to zero. In second-order perturbation theory the latter term will be accompanied by a large energy denominator, since the N^* is of order Ω above the nucleon state.

The second term in $\tilde{H}$ involves matrix elements between the nucleon state and the high-lying states. For strong coupling, this implies that the matrix elements of the second term in Eq. (4.1) go to zero rapidly because of the small overlap between the low-lying and high-lying radial wave functions. Furthermore, in perturbation theory the matrix elements of the second term will be accompanied by large energy denominators, since the low-lying states are of the order of u_1 below the high-lying states.

In summary, we expect that the second-order corrections in $\tilde{H}$ to the nucleon ground state of $H^{(0)}$ will go to zero as the bag radius goes to zero.

This completes the qualitative discussion of the perturbation corrections produced by $\tilde{H}$ in the nucleon ground state. In the next section, we explore the implications of the strong-coupling wave functions and energies by calculating some static properties of the low-lying baryons.

V. SOME STATIC PROPERTIES OF THE LOW-LYING BARYONS

Before we embark on calculations of the static properties of the low-lying baryons, we must discuss the method of specifying the free parameters of the Hamiltonian, namely, the bare mass M_0, the bare pion-nucleon coupling constant $f^{(0)}_{NN\pi}$, and the bag radius R. We can choose M_0 in Eq. (3.39) such that M_N is the physical nucleon mass. This can be done for any choice of $f^{(0)}_{NN\pi}$ and R. The value of $f^{(0)}_{NN\pi}$ is fixed by the experimental value of the renormalized pion-nucleon coupling constant, namely, $f_{NN\pi} \cong 0.29$. Instead of fixing R, we choose to plot the static properties of the baryons as a function of the bag radius.

A way of determining $f^{(0)}_{NN\pi}$ is to evaluate the expectation value of the pion field at large distances. To this end, consider the pion field expansion of Eq. (2.6),

$$\phi_\alpha(\vec{r}) = \sum_i \partial_i F(r) q_{\alpha i} + \phi'_\alpha(\vec{r}) , \tag{5.1}$$

We now add and subtract a term such that

$$\phi_\alpha(\vec{r})=\sum_{is}\partial_i F(r)B^T_{\alpha s}A_{si}(Q_s-\bar{Q}_s)+\frac{g^{(0)}}{N}\sum_i\partial_i F(r)e_{\alpha i}+\phi'_\alpha(\vec{r})\ , \tag{5.2}$$

where $\bar{Q}_s$ and $e_{\alpha i}$ are defined by Eqs. (3.24) and (4.2), respectively. Note, we have used the fact that

$$\bar{Q}_s=g^{(0)}/N \tag{5.3}$$

with N determined by Eqs. (2.8) and (2.13) and $g^{(0)}=\sqrt{4\pi}f_{NN\pi}{}^{(0)}/m_\pi$. Taking the expectation value of Eq. (5.2) with the nucleon state defined by Eq. (3.40), we obtain

$$\langle N\mid\phi_\alpha(\vec{r})\mid N\rangle=\sum_{is}\partial_i F(r)\langle N\mid B^T_{\alpha s}A_{si}(Q_s-\bar{Q}_s)\mid N\rangle-\frac{g^{(0)}}{N}\sum_i\partial_i F(r)\langle N\mid\tau_\alpha\sigma_i\mid N\rangle\ , \tag{5.4}$$

where we have used the projection theorem of Eq. (4.4) and the fact that $\langle N\mid\phi'_\alpha(\vec{r})\mid N\rangle=0$. For strong coupling, the first term in Eq. (5.4) is negligible. Substituting for $\partial_i F(r)$ from Eqs. (2.13) and (2.15) and evaluating Eq. (5.4) at large distances, say $r\gg 1/m_\pi$, we obtain

$$\langle N\mid\phi_\alpha(\vec{r})\mid N\rangle\cong\frac{g^{(0)}m_\pi}{4\pi}\frac{e^{-m_\pi r}}{r}\langle N\mid\tau_\alpha\sigma_i\hat{r}_i\mid N\rangle=\frac{Zg^{(0)}m_\pi}{4\pi}\frac{e^{-m_\pi r}}{r}\chi^\dagger\tau_\alpha\sigma_i\hat{r}_i\chi\ , \tag{5.5}$$

where Z is the renormalization constant and χ is a nucleon spin-isospinor. A straightforward calculation from Eq. (5.5) implies $Z=\frac{1}{3}$. Hence, the bare coupling constant is given by

$$f^{(0)}_{NN\pi}=3f_{NN\pi}\cong 0.85\ . \tag{5.6}$$

In Fig. 3, we plot the nucleon self-energy defined as

$$E^{(0)}_{0(1/2)(1/2)}-E_{\text{shift}}\ , \tag{5.7}$$

where $E^{(0)}_{0(1/2)(1/2)}$ and E_{shift} are given by Eqs. (3.31) and (3.37), respectively, as a function of the bag radius R. Note that the usual perturbation theory result, i.e., expanding about the free-field ground state and truncating at one pion, significantly disagrees with the strong-coupling result. From Eqs. (3.39), (3.41), and (3.42), we plot in Figs. 4 and 5 the mass differences $\Delta-N$ and N^*-N as a function of R. It is important to note that M_Δ and M^*_N in Eqs. (3.41) and (3.42) do not correspond to the physically observed masses. In order to calculate physical masses, it is necessary to solve the pion-nucleon scattering problem. The method for calculating scattering is straightforward,[10] however results will be discussed in a forthcoming publication. Therefore, Eqs. (3.41) and (3.42) should be considered estimates to the physical masses.

We now turn to a discussion of magnetic moments, charge radii, and the average number of pions in the dressed nucleon state. The total-magnetic-moment operator is given by

$$\mu_3=\mu_3^Q+\mu_3^\pi\ , \tag{5.8}$$

with the quark contribution μ_3^Q is given by

$$\mu_3^Q=(\chi_{p\uparrow}\chi^\dagger_{p\uparrow}-\chi_{p\downarrow}\chi^\dagger_{p\downarrow})u_p^{(0)}+(\chi_{n\uparrow}\chi^\dagger_{n\uparrow}-\chi_{n\downarrow}\chi^\dagger_{n\downarrow})\mu_n^{(0)}\ , \tag{5.9}$$

where $\chi_{p\uparrow}$ is a bare proton state with spin up, $\chi_{n\uparrow}\ldots$, etc, $\mu_p^{(0)}$ is the bare-proton magnetic moment given by

$$\mu_p^{(0)}=\frac{eR}{3(\omega^2-\sin^2\omega)}\left[\frac{3\omega}{2}-\frac{3}{4}\sin 2\omega-\omega\sin^2\omega\right]\ , \tag{5.10}$$

with $\omega=2.04$ and the ratio $\mu_n^{(0)}/\mu_p^{(0)}=\frac{2}{3}$. The pion contribution μ_3^π is given by

$$\mu_3^\pi=\frac{ie}{2}\int d^3r[\phi_1(\vec{r})L_3\phi_2(\vec{r})-\phi_2(\vec{r})L_3\phi_1(\vec{r})]\ , \tag{5.11}$$

where L_3 is the 3 component angular momentum $L_3=-i\epsilon_{3jk}r_j\nabla_k$.

Taking the expectation value of μ_3^Q in Eq. (5.9) with respect to the dressed proton and neutron states given by Eq. (3.40), we obtain

$$\langle p\mid\mu_3^Q\mid p\rangle=\tfrac{5}{18}\mu_p^{(0)} \tag{5.12}$$

for the proton and

$$\langle n\mid\mu_3^Q\mid n\rangle=-\tfrac{5}{18}\mu_p^{(0)} \tag{5.13}$$

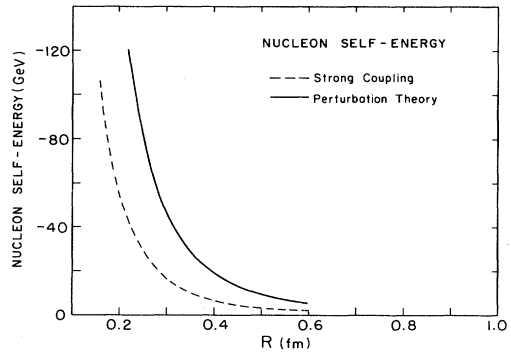

FIG. 3. A plot of the nucleon self-energy for the case of strong coupling, and compared to the standard perturbation-theory result as a function of the bag radius R.

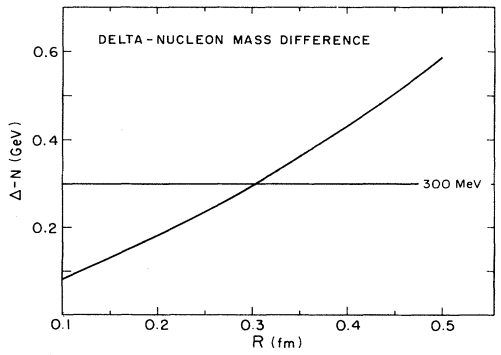

FIG. 4. A plot of the Δ-nucleon mass difference as a function of the bag radius R.

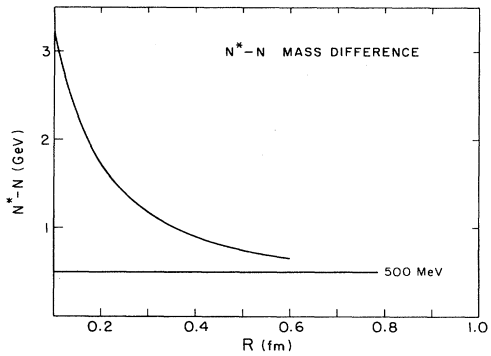

FIG. 5. A plot of the N^*-nucleon mass difference as a function of the bag radius R.

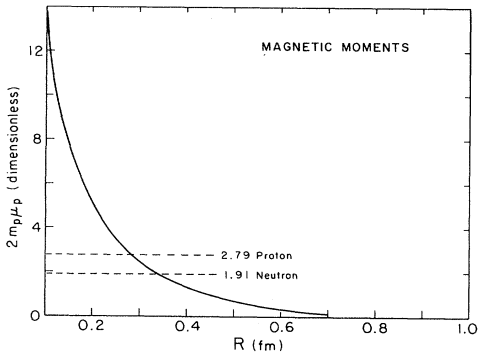

FIG. 6. A plot of the magnitude of the proton and neutron moments as a function of the bag radius R.

for the neutron. This result implies that the expectation value of the isoscalar part of μ_3^Q is zero. The origin of this result can be traced to the properties of the nucleon wave function in Eq. (3.40). As we pointed out in Sec. III A, among the eigenfunctions of Eq. (3.5) there is a singlet state with eigenvalue η_1. This state is such that the 3 components of the bare-nucleon spin and isospin are oppositely oriented. Since the isoscalar part of μ_3^Q is proportional to the bare-nucleon spin operator, then the matrix element of the isoscalar part of μ_3^Q is zero.

From the fact that the pion contribution μ_3^π is pure isovector we conclude that

$$\frac{\langle n\,|\mu_3|\,n\rangle}{\langle p\,|\mu_3|\,p\rangle}=-1\ . \tag{5.14}$$

This of course disagrees with the experimental ratio of $-\frac{2}{3}$; however, we will have more to say about this in a moment. The evaluation of the expectation value μ_3^π is instructive. Substituting Eq. (5.1) for $\phi_\alpha(\vec{r})$ into Eq. (5.11) for μ_3^π and taking matrix elements with the dressed nucleon state of Eq. (3.40), we have

$$\langle N\,|\mu_3^\pi|\,N\rangle=-e\langle N\,|(q_{11}q_{22}-q_{12}q_{21})\,|\,N\rangle\ . \tag{5.15}$$

Substituting the change of variables in Eq. (3.4) and using the cross-product relation for the A's we obtain

$$\langle N\,|\mu_3^\pi|\,N\rangle=\frac{-e}{2}\epsilon_{rsk}\epsilon_{rsj}\langle N\,|\,Q_rQ_sA_{k3}B_{j3}\,|\,N\rangle\ . \tag{5.16}$$

The angular integrations can be performed with the result that the proton and neutron matrix elements are given by

$$\langle p\,|\mu_3^\pi|\,p\rangle=\frac{e}{9}\langle W^{(0)}\,|\,Q_3\sum_i Q_i\,|\,W^{(0)}\rangle \tag{5.17}$$

and

$$\langle n\,|\mu_3^\pi|\,n\rangle=\frac{-e}{9}\langle W^{(0)}\,|\,Q_3\sum_i Q_i\,|\,W^{(0)}\rangle\ , \tag{5.18}$$

where $\langle Q_1,Q_2,Q_3\,|\,W^{(0)}\rangle=W^{(0)}$ is the radial wave function given by Eq. (D23). The remaining integrations can be performed analytically; however, the expressions are a bit messy. In Fig. 6 we plot the magnitude of the proton magnetic moment which is the sum of Eqs. (5.12) and (5.17), as a function of the bag radius. The graph makes clear the importance of the pion contribution to the nucleon magnetic moment for small bag sizes. As the bag size decreases the pion-field strength increases. This increases the pion electromagnetic current density, and therefore increases the nucleon magnetic moment. From the graph, we can see that a fit to the proton or neutron moments results in a change in the bag radius of roughly 0.02 fm. It is possible to choose the bag radius so that there is a 15% discrepancy between theory and experiment. A possible origin of this small discrepancy involves the first-order corrections to the dressed nucleon wave function due to the perturbation Hamiltonian $\tilde{H}$. Another possibility involves our neglect of the intrinsic isobar source interaction with the pion field in the CBM Hamiltonian. This interaction implies that there is an intrinsic isobar component in the dressed nucleon wave function in the lowest-order strong-coupling approximation. Furthermore, the magnetic-moment operator will contain transition operators between the bare nucleon and Δ states. The dressed-nucleon matrix element of the isoscalar part of this operator will not be zero, so that the ratio of the proton and neutron moments will not be -1.

The charge-radius calculation proceeds in a similar manner where the relevant operator is given by

$$r_{\rm ch}{}^2=eR^2\gamma(\chi_{p\uparrow}\chi_{p\uparrow}^\dagger+\chi_{p\downarrow}\chi_{p\downarrow}^\dagger)$$
$$+e\int d^3r\,r^2[\phi_1(\vec{r})\pi_2(\vec{r})-\phi_2(\vec{r})\pi_1(\vec{r})]\ , \tag{5.19}$$

where $\gamma\cong0.57$ and the $\pi_i(\vec{r})$ are the canonical momenta given by Eq. (2.7). Note there is no bare-neutron contribution from Eq. (5.19), since the up and down quarks are assumed to have equal mass and to be in an s wave.

Taking matrix elements of $r_{\rm ch}{}^2$ between the dressed proton and neutron states of Eq. (3.40), we obtain

$$\langle r^2\rangle_p=\frac{e\gamma R^2}{2}+\frac{e\beta}{2} \tag{5.20}$$

and

$$\langle r^2\rangle_n=\frac{e\gamma R^2}{2}-\frac{e\beta}{2}\ , \tag{5.21}$$

where β is given by

$$\beta=\frac{3N^2}{8\pi y^6 m_\pi}\{A^2\{y[i_0(2y)-1]-3y^2 i_1(2y)+y^3[i_0(2y)+\tfrac{1}{3}]\}+B^2(\tfrac{5}{2}+3y+y^2)e^{-2y}\} \quad (5.22)$$

with

$$y=m_\pi R\ ,$$
$$A=(1+y)e^{-y}\ ,$$
$$B=y^2 i_1(y)\ ,$$

and $i_k(y)$ the modified spherical Bessel functions. In Fig. 7 we plot the magnitude of the proton and neutron charge radii as a function of the bag radius. The charge radius of of the neutron turns out to be negative. This is due to the dominance of the π^- charge distribution surrounding the bare proton core. For a bag radius in the range 0.35 fm $>R>0.25$ fm, the neutron charge radius is within 30% of the experimental value. However, the same agreement cannot be claimed for the proton charge radius. It appears that the π^+ charge distribution surrounding the bare neutron core is not extended enough to account for the experimental value. We believe that the discrepancies between theory and experiment for the magnetic moments and charge radii are related. We are currently exploring the possibilities outlined above.

Finally, we compute the average number of pions which dress the bare nucleon core. The total-pion-number operator is given by

$$N_{\text{total}}=\sum_\mu N_\mu\ , \quad (5.23)$$

where N_μ is given by

$$N_\mu=\tfrac{1}{2}\int d^3r\,d^3r'\phi_\mu^\dagger(\vec{r})f(\vec{r},\vec{r}')\phi_\mu(\vec{r}')+\frac{i}{2}\int d^3r[\phi_\mu^\dagger(\vec{r})\pi_\mu^\dagger(\vec{r})-\pi_\mu(\vec{r})\phi_\mu(\vec{r})]+\int d^3r\,d^3r'\pi_\mu^\dagger(\vec{r})g(\vec{r},\vec{r}')\pi_\mu(\vec{r}')\ , \quad (5.24)$$

where $f(\vec{r},\vec{r}')$ is defined by Eq. (3.38) and $g(\vec{r},\vec{r}')$ is the inverse of $f(\vec{r},\vec{r}')$ given by

$$g(\vec{r},\vec{r}')=\int\frac{d^3k}{(2\pi)^3}\frac{e^{i\vec{k}(\vec{r}-\vec{r}')}}{\omega(k)}\ , \quad (5.25)$$

and the fields ϕ_μ and π_μ are defined by

$$\phi_+=\frac{\phi_1+i\phi_2}{\sqrt{2}},\quad \pi_+=\frac{\pi_1-i\pi_2}{\sqrt{2}}\ ,$$
$$\phi_-=\frac{\phi_1-i\phi_2}{\sqrt{2}},\quad \pi_-=\frac{\pi_1+i\pi_2}{\sqrt{2}}\ , \quad (5.26)$$
$$\phi_0=\phi_3,\quad \pi_0=\pi_3\ ,$$

where $\mu=+,0,-$. The expression for N_μ in Eq. (5.24) may be unfamiliar; however, it can be derived from the usual free-field expression.

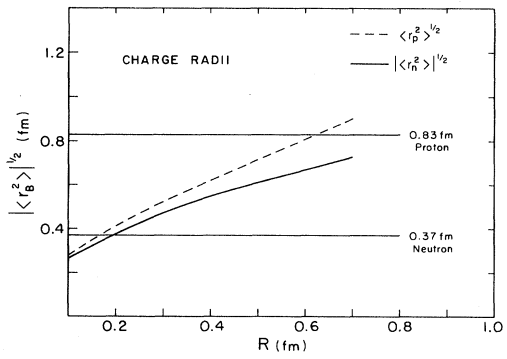

FIG. 7. A plot of the magnitude of the proton and neutron charge radii as a function of the bag radius R.

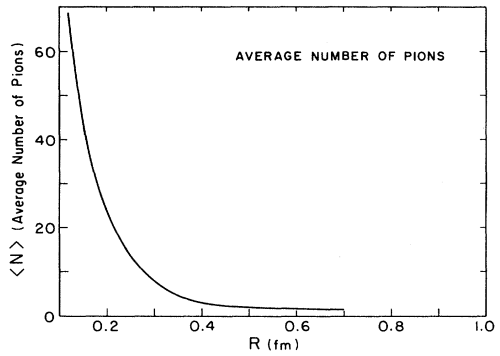

FIG. 8. A plot of the average number of pions in the dressed nucleon state as a function of the bag radius R.

In Fig. 8. we plot the expectation value of N_{total} with respect to the dressed nucleon wave function defined by Eq. (3.40). The increase in the number of pions as the bag radius decreases is an important feature of the model and a signal that the pion coupling to the nucleon source is strong. As a further justification for the strong-coupling approximation, we observe that the average number of pions is approximately 6 for a bag radius of 0.3 fm.

VI. CONCLUSIONS

We have argued that for a bag radius of the order of the proton Compton wavelength the pion-nucleon coupling described by Eq. (2.1) is strong and a discussion of the energy content of the system requires a nonperturbative quantum-mechanical computational scheme. Our results for the static properties of the low-lying baryons involve a bag radius which is consistent with the strong-coupling approximation. However, our lowest-order results for the ratio of the neutron and proton magnetic moments and charge radii are somewhat disappointing. For example, our lowest-order calculation of the ratio of magnetic moments is -1, which is roughly in 30% disagreement with experiment. However, we have shown that a significant part of this ratio can be accounted for by the isovector contribution from pions. In order to improve the lowest-order results we need an isoscalar contribution from the

bare-bag magnetic-moment operators in Eq. (5.9). A way of generating such a contribution involves an improvement in the nucleon wave function, namely, computing first-order corrections produced by the perturbations. This can be done since we now have a systematic method for correcting the strong-coupling approximation. Another way of improvement involves an application of the strong-coupling approximation to the CBM Hamiltonian which includes the interaction of the pion field with the intrinsic isobar source. This interaction implies an intrinsic isobar component in the dressed nucleon wave function in the lowest-order strong-coupling approximation. Furthermore, the magnetic-moment operator will contain transition operators between the bare-bag nucleon and Δ states. The dressed-nucleon matrix element of the isoscalar part of this operator will not be zero, so that the ratio of the proton and neutron moments will not be -1. In contrast to the previous way of generating an isoscalar contribution, this approach emphasizes the role of the intrinsic isobar, and hence the quark degrees of freedom.

We believe that the discrepancies between theory and experiment for the magnetic moments and radii are related. We are currently exploring the possibilities outlined above.

ACKNOWLEDGMENTS

The author would like to thank the Andrew Mellon Foundation and the National Science Foundation for financial support. The author is especially grateful to C. M. Vincent for his clear thinking, his insightful ideas, and many stimulating conversations over the past year. The author is also grateful to F. Coester for suggesting the problem for many discussions of the strong-coupling approximation in quantum field theory.

APPENDIX A

We discuss implications of the change of variables defined by Eq. (3.4), in particular the parameter space of the Euler angles and radial variables. For the moment we consider a simpler problem involving four Cartesian variables $q_{\alpha i}$, where $\alpha,i=1,2$ so that Eq. (3.4) becomes

$$\begin{bmatrix} q_{11} & q_{12} \\ q_{21} & q_{22} \end{bmatrix} = \begin{bmatrix} \cos\Phi & -\sin\Phi \\ \sin\Phi & \cos\Phi \end{bmatrix} \begin{bmatrix} Q_1 & 0 \\ 0 & Q_2 \end{bmatrix} \times \begin{bmatrix} \cos\phi & \sin\phi \\ -\sin\phi & \cos\phi \end{bmatrix} . \tag{A1}$$

From the $q_{\alpha i}$ one can construct two rotationally invariant quantities given by

$$S_1=\sum_{\alpha i} q_{\alpha i}{}^2=Q_1{}^2+Q_2{}^2 \tag{A2}$$

and

$$S_2=\det q=Q_1Q_2 . \tag{A3}$$

The parameter space of the $q_{\alpha i}$, namely, $\infty>q_{\alpha i}>-\infty$, implies that

$$\begin{aligned} &\infty>S_1\geq 0 , \\ &\infty>S_2>-\infty . \end{aligned} \tag{A4}$$

However, from Eqs. (A2) and (A3) one can show that

$$S_1{}^2-4S_2{}^2\geq 0 , \tag{A5}$$

which implies that S_1 and S_2 cannot vary independently.

For a given S_1 and S_2, it is possible to solve Eqs. (A2) and (A3) for Q_1 and Q_2. The result is a set of solutions given by

$$Q_1=\pm\left[\frac{S_1\pm(S_1{}^2-4S_2{}^2)^{1/2}}{2}\right]^{1/2} , \tag{A6}$$

$$Q_2=\pm\mathrm{sgn}(S_2)\left[\frac{S_1\mp(S_1{}^2-4S_2{}^2)^{1/2}}{2}\right]^{1/2} . \tag{A7}$$

Geometrically, Eq. (A2) describes a circle for fixed S_1 and Eq. (A3) a hyperbola for fixed S_2. If we allow $\infty>Q_1,Q_2>-\infty$, then there are four hyperbolas. The solutions in Eqs. (A6) and (A7) correspond to the points of intersection of the circle and the four hyperbolas. The existence of multiple solutions implies that there are redundant regions in the parameter space of Q_1 and Q_2. There are four redundant regions and we want to pick one of them. A choice, which satisfies the condition $\infty>S_2>-\infty$, is given by

$$\infty>Q_1\geq|Q_2|\geq 0 . \tag{A8}$$

This is the region bounded by the lines $Q_1=Q_2$ and $Q_2=-Q_1$ with $Q_1\geq 0$.

The integration measure associated with the transformation defined by Eq. (A1) is given by the Jacobian of the transformation. A straightforward calculation of the magnitude of the Jacobian gives

$$|J|=Q_1{}^2-Q_2{}^2 . \tag{A9}$$

Combining Eqs. (A8) and (A9), we can write the equivalence of volume integrals in the form

$$\int_{-\infty}^{\infty}\prod_{\alpha i} dq_{\alpha i}=\int_{\{P\}} d\phi\, d\Phi \int_0^{\infty} dQ_1 \int_{-Q_1}^{Q_1} dQ_2 (Q_1{}^2-Q_2{}^2) , \tag{A10}$$

where $\{P\}$ is the parameter space of the angles ϕ and Φ. In order to determine $\{P\}$, we define a matrix $q'_{\alpha i}$ such that

$$q'=B^T b^T Q a A , \tag{A11}$$

where b^T and a are 2×2 proper orthogonal matrices which by assumption are independent of the Q_r and B^T, A, and Q are the matrices defined by Eq. (A1). We now require that

$$q'=q , \tag{A12}$$

where q is given by Eq. (A1). From the orthogonality of the A and B matrices we obtain

$$b^T Q a=Q . \tag{A13}$$

Equation (A12) is true for all values of the Q_r's, in partic-

ular $Q_1=Q_2$ which implies that Q is proportional to the unit matrix. This fact and the orthogonality of b implies that $a=b$, hence from Eq. (A12) we have

$$[b,Q]=0\ . \tag{A14}$$

Therefore, b can be simultaneously diagonalized with Q so that b is of the form

$$b=\begin{bmatrix} b_1 & 0 \\ 0 & b_2 \end{bmatrix}\ . \tag{A15}$$

The orthogonality of b implies that the eigenvalues are given by

$$\begin{aligned} b_1&=\pm 1\ , \\ b_2&=\pm 1\ . \end{aligned} \tag{A16}$$

Hence there are two proper orthogonal matrices of the form

$$b=\begin{bmatrix} 1 & 0 \\ 0 & 1 \end{bmatrix},\quad \begin{bmatrix} -1 & 0 \\ 0 & -1 \end{bmatrix}\ . \tag{A17}$$

The identity matrix is uninteresting; however, the second solution implies that the $q_{\alpha i}$ are invariant with respect to simultaneous body-fixed rotations of the form

$$\begin{aligned} \Phi&\rightarrow\Phi\pm\pi\ , \\ \phi&\rightarrow\phi\pm\pi\ . \end{aligned} \tag{A18}$$

If we assume $2\pi\geq\phi$, $\Phi\geq 0$, then the transformations expressed by (A18) imply that there are redundant regions of integration in Eq. (A10). It is straightforward to show that the region of integration $2\pi\geq\phi$, $\Phi\geq 0$ is twice $\{P\}$,[19] which is given by

$$\begin{aligned} &2\pi\geq\phi\geq 0\ , \\ &\pi\geq\Phi\geq 0\ . \end{aligned} \tag{A19}$$

A similar analysis can be carried out for the nine-dimensional case of Eq. (3.4); however, we will just outline the steps. In this case there are three invariants given by

$$\begin{aligned} S_1&=\sum_{\alpha i} q_{\alpha i}{}^2=Q_1{}^2+Q_2{}^2+Q_3{}^2\ , \\ S_2&=\det q=Q_1Q_2Q_3\ , \\ S_3&=\sum_{\substack{\alpha i \\ \beta j}} q_{\alpha i}q_{\beta j}q_{\alpha j}q_{\beta i}=Q_1{}^4+Q_2{}^4+Q_3{}^4\ . \end{aligned} \tag{A20}$$

An analytic solution of the Q_r's in terms of the S_i's is possible but not useful; however, the three geometries of Eqs. (A19) correspond to a sphere, eight hyperbolic sheets (one in each octant), and a "cube" with rounded edges. Again in the Q_1, Q_2, and Q_3 space there are redundant regions. The regions can be determined graphically by plotting planar slices of the three geometries and determining the points of intersection. A choice of the radial parameter space which is covered once is given by

$$\infty>Q_1\geq Q_2\geq|Q_3|\geq 0\ , \tag{A21}$$

which is the tetrahedron in Fig. 1. The measure of the transformation can be obtained by standard methods[20] and is given by Eqs. (3.10). The discrete transformation matrices which correspond to Eq. (A17) are the proper orthogonal matrices given by

$$\begin{aligned} b=&\begin{bmatrix} 1 & 0 & 0 \\ 0 & 1 & 0 \\ 0 & 0 & 1 \end{bmatrix},\quad \begin{bmatrix} -1 & 0 & 0 \\ 0 & -1 & 0 \\ 0 & 0 & 1 \end{bmatrix}, \\ &\begin{bmatrix} -1 & 0 & 0 \\ 0 & 1 & 0 \\ 0 & 0 & -1 \end{bmatrix},\quad \begin{bmatrix} 1 & 0 & 0 \\ 0 & -1 & 0 \\ 0 & 0 & -1 \end{bmatrix}\ . \end{aligned} \tag{A22}$$

Of the four rotation matrices only two are independent. We will select the second and third in Eq. (A22), which correspond to the transformations

$$\begin{aligned} &\psi\rightarrow\psi\pm\pi\ , \\ &\Psi\rightarrow\Psi\pm\pi \end{aligned} \tag{A23}$$

and

$$\begin{aligned} &\theta\rightarrow\theta\pm\pi,\quad \psi\rightarrow-\psi\ , \\ &\Theta\rightarrow\Theta\pm\pi,\quad \Psi\rightarrow-\Psi\ , \end{aligned} \tag{A24}$$

respectively. The unitary operators which induce these transformations on the Hilbert space of states of the collective Hamiltonian H_c are given by

$$V_3=e^{\pm i\pi(\hat{L}_3+\hat{T}_3)}\ , \tag{A25}$$

and

$$V_2=e^{\pm i\pi(\hat{L}_2+\hat{T}_2)}\ , \tag{A26}$$

where $\hat{L}_i$ and $\hat{T}_\alpha$ are the body-fixed rotation operators given by Eq. (3.16). The existence of V_2 and V_3 imply that the eigenfunctions of H_c must be invariant with respect to the discrete transformations of Eqs. (A23) and (A24). These unitary operators are important for the construction of wave functions which will be discussed in Appendices B and C.

The transformations of (A23) and (A24) imply that the standard choice for the parameter space of the two sets of Euler angles $\{\phi,\theta,\psi\}$ and $\{\Phi,\Theta,\Psi\}$ is redundant. As before, one can show that the region of integration[19] of the Euler angles is given by

$$\begin{aligned} &2\pi\geq\phi\geq 0,\quad \pi\geq\Phi\geq 0\ , \\ &2\pi\geq\psi\geq 0,\quad \pi\geq\Psi\geq 0\ , \\ &\pi\geq\theta\geq 0,\quad \pi\geq\Theta\geq 0\ . \end{aligned} \tag{A27}$$

Hence, the equivalence of volume integrals is given by Eq. (3.11).

APPENDIX B

We discuss the implications of the discrete transformations in Eqs. (A23) and (A24) for the basis states of Eq. (3.19). For a rotation of π the unitary operators in Eqs.

(A25) and (A26) can be written in the form

$$V_3=-\hat{\sigma}_3\hat{\tau}_3 e^{-i\pi(\hat{J}_3+\hat{I}_3)}\,,$$
$$V_2=-\hat{\sigma}_2\hat{\tau}_2 e^{-i\pi(\hat{J}_2+\hat{I}_2)}\,, \tag{B1}$$

where $\hat{J}_i$, $\hat{I}_\alpha$, etc., are given by Eqs. (3.16) and (3.17). Now define a set of states such that

$$|\Psi,\eta_i\rangle=\sum_{\{\hat{j}_z,\hat{i}_z\}} W_{\hat{j}_z\hat{i}_z\eta_i}\,|j^c,j_z^c,\hat{j}_z;i^c,i_z^c,\hat{i}_z;\eta_i\rangle\,, \tag{B2}$$

then $|\Psi\rangle$ defined by Eq. (3.19) is given by

$$|\Psi\rangle=\sum_{\eta_i}|\Psi,\eta_i\rangle\,. \tag{B3}$$

Note that the states $|\Psi,\eta_i\rangle$ in Eq. (B2) are eigenfunctions of the $\hat{\sigma}_r\hat{\tau}_r$. This follows from Eqs. (3.3), (3.4), and the discussion leading up to Eqs. (3.8). If we apply V_3 to $|\Psi,\eta_i\rangle$, we obtain

$$V_3|\Psi,\eta_i\rangle=-\hat{\sigma}_3\hat{\tau}_3\sum_{\{\hat{j}_z,\hat{i}_z\}} W_{\hat{j}_z\hat{i}_z\eta_i}e^{-i\pi(\hat{j}_z+\hat{i}_z)}\,|j^c,j_z^c,\hat{j}_z;i^c,i_z^c,\hat{i}_z;\eta_i\rangle\,. \tag{B4}$$

If $i=1$, then the eigenvalue of $\hat{\sigma}_3\hat{\tau}_3$ is -1 and Eq. (B4) becomes

$$V_3|\Psi,\eta_1\rangle=\sum_{\{\hat{j}_z,\hat{i}_z\}} W_{\hat{j}_z\hat{i}_z\eta_1}(-1)^{\hat{j}_z+\hat{i}_z}\,|j^c,j_z^c,\hat{j}_z;i^c,i_z^c,\hat{i}_z;\eta_1\rangle\,. \tag{B5}$$

If $|\Psi,\eta_1\rangle$ is invariant under V_3, then Eq. (B5) implies

$$W_{\hat{j}_z\hat{i}_z\eta_1}=(-1)^{\hat{j}_z+\hat{i}_z}W_{\hat{j}_z\hat{i}_z\eta_1}\,. \tag{B6}$$

For the case of the V_2 transformation we obtain from Eq. (B2) the relation

$$W_{\hat{j}_z\hat{i}_z\eta_1}=(-1)^{j^c+i^c}(-1)^{3(\hat{j}_z+\hat{i}_z)}W_{-\hat{j}_z-\hat{i}_z\eta_1}\,. \tag{B7}$$

For $j^c=i^c=\frac{1}{2}$, Eqs. (B6) and (B7) imply that $|\Psi,\eta_1\rangle$ in Eq. (B2) is given by

$$|\Psi,\eta_1\rangle=W_{\eta_1}(|\tfrac{1}{2},j_z^c,\tfrac{1}{2};\tfrac{1}{2},i_z^c,-\tfrac{1}{2};\eta_1\rangle-|\tfrac{1}{2},j_z^c-\tfrac{1}{2};\tfrac{1}{2},i_z^c,\tfrac{1}{2};\eta_1\rangle)\,, \tag{B8}$$

where we have suppressed the angular momentum labels, etc., on W_1. Finally the case of $j^c=\frac{1}{2}$ and $i^c=\frac{3}{2}$ with $\eta_i=\eta_1$ involves two W's while $j^c=i^c=\frac{3}{2}$ involves four W's. This feature has implications for the nature of the energy spectrum of H_c in the strong-coupling approximation. We will have more to say about this in Appendix C.

APPENDIX C

The eigenfunctions of Eq. (3.5), namely, $u|\Lambda,\eta_1\rangle$ are straightforward to obtain since the eigenvalues η_i are given by Eqs. (3.8). Let these eigenvectors be denoted by $|\lambda_i\rangle$, then the eigenfunctions in Eq. (3.3) are given by

$$|\Lambda,\eta_i\rangle=u^{-1}|\lambda_i\rangle\,, \tag{C1}$$

where u is defined by Eqs. (3.6) and (3.7). The $|\lambda_i\rangle$ depend on the bare-nucleon spin-isospinors and have a functional dependence on the Euler angles $\{\phi,\theta,\psi\}$ and $\{\Phi,\Theta,\Psi\}$. This functional dependence is determined by the following eigenvalue equations:

$$\begin{aligned}
&(\vec{J}^{\,c})^2|\Lambda,\eta_i\rangle=j^c(j^c+1)|\Lambda,\eta_i\rangle\,,\\
&J_3^c|\Lambda,\eta_i\rangle=j_z^c|\Lambda,\eta_i\rangle\,,\\
&\hat{J}_3|\Lambda,\eta_i\rangle=\hat{j}_z|\Lambda,\eta_i\rangle\,,\\
&(\vec{I}^{\,c})^2|\Lambda,\eta_i\rangle=i^c(i^c+1)|\Lambda,\eta_i\rangle\,,\\
&I_3^c|\Lambda,\eta_i\rangle=i_z^c|\Lambda,\eta_i\rangle\,,\\
&\hat{I}_3|\Lambda,\eta_i\rangle=\hat{i}_z|\Lambda,\eta_i\rangle\,,
\end{aligned} \tag{C2}$$

where the symmetry operators are defined by Eqs. (3.17) and the quantum numbers $\Lambda=(j^c,j_z^c,\hat{j}_z;i^c,i_z^c,\hat{i}_z)$. The representation of the symmetry operators in terms of Euler angles has been discussed by Pauli and Dancoff. The solutions to Eqs. (C2) involve Wigner functions[21] in spin and isospin space. We will not present a complete set of solutions to Eqs. (C2); however, a particular subset, which is relevant to the low-lying wave function in Eq. (B8), will be discussed. The angular part of the low-lying wave function for the case of $j_z^c=i_z^c=\frac{1}{2}$ is given by

$$|\tfrac{1}{2},\tfrac{1}{2},\tfrac{1}{2};\tfrac{1}{2},\tfrac{1}{2},-\tfrac{1}{2};\eta_1\rangle-|\tfrac{1}{2},\tfrac{1}{2},-\tfrac{1}{2};\tfrac{1}{2},\tfrac{1}{2},\tfrac{1}{2};\eta_1\rangle=\frac{1}{2}\left[\begin{bmatrix}d^{*(0)}_{00}\\0\end{bmatrix}_\sigma\begin{bmatrix}D^{*(0)}_{00}\\0\end{bmatrix}_\tau-\begin{bmatrix}d^{*(0)}_{00}\\-\sqrt{2}\,d^{*(1)}_{10}\end{bmatrix}_\sigma\begin{bmatrix}D^{*(1)}_{00}\\-\sqrt{2}\,D^{*(1)}_{10}\end{bmatrix}_\tau\right.$$
$$+\begin{bmatrix}d^{*(1)}_{0-1}\\-\sqrt{2}\,d^{*(1)}_{1-1}\end{bmatrix}_\sigma\begin{bmatrix}D^{*(1)}_{01}\\-\sqrt{2}\,D^{*(1)}_{11}\end{bmatrix}_\tau$$
$$\left.+\begin{bmatrix}d^{*(1)}_{01}\\-\sqrt{2}\,d^{*(1)}_{11}\end{bmatrix}_\sigma\begin{bmatrix}D^{*(1)}_{0-1}\\-\sqrt{2}\,D^{*(1)}_{1-1}\end{bmatrix}_\tau\right], \tag{C3}$$

where the subscripts σ and τ on the spinors refer to spin and isospin space, respectively. The d^* and D^* are Wigner functions which depend on the Euler angles $\{\phi,\theta,\psi\}$ and $\{\Phi,\Theta,\Psi\}$, respectively. The angular wave function defined by Eq. (C3) describes the dynamical coupling of the bare-nucleon spin and isospin degrees of freedom to the spin and isospin degrees of freedom of the pion field. The angular wave function in Eq. (C3) and the radial function W_{η_1} completely specify the form of the low-lying wave function in Eq. (B8).

In order to completely determine the low-lying wave function, we must operate with the collective Hamiltonian H_c defined by Eq. (3.14) on the wave function defined by Eq. (B8) and take matrix elements. The only operator in H_c which presents some difficulty is the centrifugal barrier H_{cb} defined by Eq. (3.15). Employing the Wigner-Eckart theorem for body-fixed angular momentum and isospin operators the matrix element of H_{cb} between the angular wave functions defined by Eq. (C3) is given by

$$\langle H_{cb}\rangle=2\sum_{r<s}\frac{1}{(Q_r+Q_s)^2}\ . \tag{C4}$$

For the case when $j^c=i^c=\frac{3}{2}$, evaluation of the matrix elements of H_{cb} is not so simple, since the form of $|\Psi,\eta_1\rangle$ involves four radial wave functions. Each radial wave function is multiplied by an angular wave function which can be formed out of the solutions to Eqs. (C2). In this four-dimensional space, the centrifugal barrier H_{cb} is a 4×4 matrix which can be diagonalized analytically. The lowest eigenvalue is given by

$$\langle H_{cb}\rangle=12\sum_{r<s}\frac{1}{(Q_r+Q_s)^2}\ . \tag{C5}$$

The other three eigenvalues are higher in energy since they involve both $1/(Q_r-Q_s)^2$ and $1/(Q_r+Q_s)^2$ terms. Spectroscopically, this implies that there are four sets of low-lying energy levels with $j^c=i^c=\frac{3}{2}$. This clearly indicates that the collective Hamiltonian H_c has an incredibly rich spectrum.

APPENDIX D

The eigenvalue equation we want to solve is of the form

$$h_0W^{(0)}=E^{(0)}W^{(0)}\ , \tag{D1}$$

where h_0 is given by Eq. (3.29). We define a set of dimensionless variables such that

$$x_r=\frac{\sqrt{\Omega}}{2}Q_r\ ; \tag{D2}$$

then Eq. (D1) can be written

$$\left\{\sum_r\left[-\frac{1}{2}\frac{\partial^2}{\partial x_r{}^2}+2x_r{}^2-\left[\frac{2}{\Omega}\right]^{3/2}g^{(0)}\lambda x_r\right]-\frac{1}{2}\sum_{r<s}\frac{1}{x_r-x_s}\left[\frac{\partial}{\partial x_r}-\frac{\partial}{\partial x_s}\right]\right\}W^{(0)}=\epsilon^{(0)}W^{(0)}\ , \tag{D3}$$

where $\epsilon^{(0)}=E^{(0)}/2\Omega$. We define a reduced wave function $\omega^{(0)}$ such that

$$W^{(0)}=\frac{\omega^{(0)}}{G}\ , \tag{D4}$$

where $G=(x_1-x_2)^{1/2}(x_1-x_3)^{1/2}(x_2-x_3)^{1/2}$. Then $\omega^{(0)}$ satisfies

$$\left\{\sum_r\left[-\frac{1}{2}\frac{\partial}{\partial x_r{}^2}+2x_r{}^2-\left[\frac{2}{\Omega}\right]^{3/2}g^{(0)}\lambda x_r\right]-\frac{1}{4}\sum_{r<s}\frac{1}{(x_r-x_s)^2}\right\}\omega^{(0)}=\epsilon^{(0)}\omega^{(0)}\ . \tag{D5}$$

Geometrically, the singularities of Eq. (D5) are located on the planes $x_1=x_2$ and $x_2=x_3$, and the line $x_1=x_2=x_3$ in Fig. 1. Since the wave function $\omega^{(0)}$ is localized somewhere along this line, it is convenient to rotate the x_3 axis onto the line and the x_2 axis into the plane $x_1=x_2$. This rotational transformation is given by

$$x_1=\frac{\sqrt{2}}{3}x_1'+\frac{1}{\sqrt{3}}x_3' ,$$
$$x_2=-\frac{1}{\sqrt{6}}x_1'+\frac{1}{\sqrt{2}}x_2'+\frac{1}{\sqrt{3}}x_3' , \tag{D6}$$
$$x_3=-\frac{1}{\sqrt{6}}x_1'-\frac{1}{\sqrt{2}}x_2'+\frac{1}{\sqrt{3}}x_3' ,$$

which upon substitution in Eq. (D5) gives

$$\left\{\sum_r\left[-\frac{1}{2}\frac{\partial}{\partial x_r'^2}+2x_r'^2\right]-\sqrt{3}\left[\frac{2}{\Omega}\right]^{3/2}g^{(0)}\lambda x_3'-\frac{1}{4}\left[\frac{2}{(\sqrt{3}x_1'-x_2')^2}+\frac{2}{(\sqrt{3}x_1'+x_2')^2}+\frac{1}{2x_2'^2}\right]\right\}\omega^{(0)}=\epsilon^{(0)}\omega^{(0)} . \tag{D7}$$

The linear-coupling term can be transformed away by the change of variables given by

$$z_1=x_1' ,$$
$$z_2=x_2' , \tag{D8}$$
$$z_3=x_3'-x_0 ,$$

where

$$x_0=\frac{\sqrt{3}}{4}\left[\frac{2}{\Omega}\right]^{3/2}g^{(0)}\lambda , \tag{D9}$$

hence Eq. (D7) becomes

$$\left[\sum_r\left[-\frac{1}{2}\frac{\partial}{\partial z_r^2}+2z_r^2\right]-\frac{1}{4}\left[\frac{2}{(\sqrt{3}z_1-z_2)^2}+\frac{2}{(\sqrt{3}z_1+z_2)}+\frac{1}{2z_2^2}\right]\right]\omega^{(0)}=\tilde{\epsilon}^{(0)}\omega^{(0)} , \tag{D10}$$

where $\tilde{\epsilon}^{(0)}=\epsilon^{(0)}+2x_0^2$. From Eqs. (D8) we observe that x_0 is a measure of the displacement of the radial wave function $\omega^{(0)}$ along the line $x_1=x_2=x_3$. As x_0 increases the radial wave function moves further away from the less important singularities at the origin $x_1=x_2=x_3=0$ on the plane $x_1=-x_3$, and along the line $x_3=-x_1=-x_2$.

If we go to cylindrical coordinates, then $\omega^{(0)}$ separates such that

$$\omega^{(0)}=R(\rho)B(\beta)Z(z_3) . \tag{D11}$$

where $R(\rho)$, $B(\beta)$, and $Z(z_3)$ satisfy

$$-\tfrac{1}{2}Z''+2z_3^2Z=kZ , \tag{D12}$$

and

$$\left[-\frac{d^2}{d\beta^2}-\frac{1}{2}\left[\frac{2}{(\sqrt{3}\cos\beta-\sin\beta)^2}+\frac{2}{(\sqrt{3}\cos\beta+\sin\beta)^2}+\frac{1}{2\sin^2\beta}\right]\right]B=lB \tag{D13}$$

and

$$\left[-\frac{1}{2}\left[\frac{d^2}{d\rho^2}+\frac{1}{\rho}\frac{d}{d\rho}\right]+2\rho^2+\frac{l}{2\rho^2}\right]R=mR , \tag{D14}$$

where k, l, and m are quantum numbers to be determined, $\rho=(z_1^2+z_2^2)^{1/2}$, and the angle β is bounded by the two intersecting planes $x_2=x_3$ and $x_1=x_2$ such that $\pi/3\geq\beta\geq 0$. The eigenvalue $\tilde{\epsilon}^{(0)}$ is given by

$$\tilde{\epsilon}^{(0)}=k+m . \tag{D15}$$

For a small bag radius or strong coupling the parameter spaces of z_3 and ρ are well approximated by

$$\infty>\rho\geq 0 ,$$
$$\infty>z_3>-\infty , \tag{D16}$$

since x_0 in Eq. (D9) tends to infinity in the limit when the bag radius goes to zero. Under these conditions, Eq. (D12) is a one-dimensional harmonic oscillator with solutions of the form

$$Z(z_3)=e^{-z_3^2}H_n(\sqrt{2}z_3) , \tag{D17}$$

and k in Eq. (D12) is given by

$$k=2n+1 , \tag{D18}$$

where H_n are Hermite polynomials. We have not been able to find a general solution to Eq. (D13); however, the lowest eigenfunction and eigenvalue are given by

$$B(\beta)=(\cos\beta'-\sqrt{3}\sin\beta')^{1/2}$$
$$\times(\cos\beta'+\sqrt{3}\sin\beta')^{1/2}(\cos\beta')^{1/2} , \tag{D19}$$

where $\beta'=\beta-\pi/6$ and l in Eq. (D13) is given by

$$l=\frac{9}{4} . \tag{D20}$$

Finally, substituting Eq. (D20) into Eq. (D14) and recognizing that Eq. (D14) is related to a two-dimensional oscillator equation, we obtain

$$R=e^{-\rho^2}\rho^2 L_p^{(3/2)}(2\rho^2) . \tag{D21}$$

Hence, m in Eq. (D14) is given by

$$m=(4p+5) , \tag{D22}$$

which completes the determination of $W^{(0)}$ and $E^{(0)}$ in Eq. (D1). In summary, we have wave functions given by

$$W^{(0)}_{pln}=R_p(\rho)B_l(\beta)Z_n(z_3)/G , \tag{D23}$$

which for $l=\frac{9}{4}$ have eigenvalues given by

$$E^{(0)}_{p(9/4)n}=\frac{\Omega}{2}(4p+2n+6)-\Omega x_0^2 . \tag{D24}$$

The lowest eigenvalue has $p=n=0$ and the next highest eigenvalue has $p=0$ and $n=1$. The first-order energy shift involves matrix elements of h'_{cb} in Eq. (3.30). In terms of the x_r variables in Eq. (D2) h'_{cb} is given by

$$h'_{cb}=\frac{\Omega}{4}\sum_{r<s}\frac{1}{(x_r+x_s)^2} . \tag{D25}$$

To obtain the first-order energy shift we expand h'_{cb} about the point $x_1=x_2=x_3=x_0$ and keep the leading term. The results for the two lowest eigenvalues of the collective Hamiltonian H_c in the strong-coupling approximation are given by Eqs. (3.31) and (3.32). Note that the first subscript refers to the n quantum number of Eq. (D18). Other quantum labels such as l and p have been suppressed since they are the same for the two lowest eigenvalues. Furthermore, the low-lying wave function $|\Psi,\eta_1\rangle$ is approximately given by

$$|\Psi,\eta_1\rangle\cong|\Psi^{(0)},\eta_1\rangle W^{(0)}(\,|\tfrac{1}{2},j_z^c,\tfrac{1}{2};\tfrac{1}{2},i_z^c-\tfrac{1}{2};\eta_1\rangle - |\tfrac{1}{2},j_z^c,-\tfrac{1}{2};\tfrac{1}{2},i_z^c,\tfrac{1}{2};\eta_1\rangle) , \tag{D26}$$

where $W^{(0)}$ is given by Eq. (D23).

---

*Present address.

[1]A. Chodos and C. B. Thorn, Phys. Rev. D 12, 2733 (1975); T. Inoue and T. Maskawa, Prog. Theor. Phys. 54, 1933 (1975).

[2]A. W. Thomas, S. Theberge, and G. A. Miller, Phys. Rev. D 22, 2838 (1980); 23, 2106(E) (1981); G. A. Miller, A. W. Thomas, and S. Theberge, Phys. Lett. 91B, 192 (1980); S. Theberge, A. W. Thomas, and G. A. Miller, Phys. Rev. D 24, 216 (1981); S. Theberge and A. W. Thomas, *ibid.* 25, 284 (1982); S. Theberge, G. A. Miller, and A. W. Thomas, Can. J. Phys. 60, 59 (1982).

[3]G. E. Brown and M. Rho, Phys. Lett. 82B, 177 (1979); G. E. Brown, M. Rho, and V. Vento *ibid.* 84B, 383 (1970); V. Vento, M. Rho, E. M. Nyman, J. H. Jun, and G. E. Brown, Nucl. Phys. A345, 413 (1980); F. Myhrer, G. E. Brown, and Z Xu. *ibid.* A362, 317 (1981).

[4]C. Callen, R. Dashen, and D. Gross, Phys. Rev. D 19, 1826 (1979).

[5]C. E. DeTar, Phys. Rev. D 24, 752 (1980); 24, 762 (1980).

[6]M. Lacombe, B. Loiseau, J. M. Richard, R. Vinh Mau, J. Cote, P. Pires, and R. de Tourreil Phys. Rev. C 21, 861 (1980); R. Vinh Mau, Nucl. Phys. A335, 211 (1980); A328, 381 (1979), and references therein.

[7]A. Chodos, R. L. Jaffe, K. Johnson, C. B. Thorn, and V. F. Weisskopf, Phys. Rev. D 9, 3471 (1974); A. Chodos, R. L. Jaffe, K. Johnson, and C. B. Thorn, Phys. Rev. D 10, 2599 (1974); T. De Grand, R. L. Jaffe, K. Johnson, and J. Kiskis, Phys. Rev. D 12, 2060 (1975).

[8]J. Carlson and V. R. Pandharipande, Nucl. Phys. A371, 301 (1981); G. L. Payne, J. L. Friar, and B. F. Gibson, Phys. Rev. C 22, 832 (1980); Ch. Hajduk and P. U. Sauer, Nucl. Phys. 369, 321 (1981); A. Laverne and C. Gignoux, *ibid.* A203, 597 (1973); W. Glockle, *ibid.* A301, 343 (1982); Y. E. Kim and A. Tubis, Annu. Rev. Nucl. Sci. 24, 69 (1974).

[9]P. Hoodbhoy, Phys. Rev. D 26, 3235 (1982).

[10]J. A. Parmentola, Phys. Rev. D 27, 2686 (1983).

[11]The earliest reference on the strong-coupling approximation is G. Wentzel, Helv. Phys. Acta 13, 269 (1940).

[12]The so-called static Chew model was first discussed in the strong-coupling approximation by W. Pauli and S. M. Dancoff, Phys. Rev. 62, 851 (1942).

[13]K. G. Wilson, Phys. Rev. 140, 445 (1965); Phys. Rev. D 2, 1438 (1970).

[14]Strictly speaking for CBM, $f^{(0)}_{NN\pi}$ is not a free parameter; however, for phenomenological applications it must be considered a free parameter because of renormalization effects.

[15]M. Bolsterli, Phys. Rev. D 24, 400 (1981); 25, 1095 (1982), and references therein.

[16]C. Schwartz, Phys. Rev. 137, 2120 (1965).

[17]Unfortunately, the answer to the question "λ large compared to what?" requires further discussion of the collective Hamiltonian in Eq. (2.17). However, the quantity with dimensions that λ is to be compared to is

$$\left[\frac{\sqrt{3}}{4}\left[\frac{2}{\Omega}\right]^{3/2}g^{(0)}\right]^{-1} .$$

This quantity enters into the definition of a dimensionless quantity x_0 which is defined by Eq. (D9). The significance of x_0 is discussed in Sec. III A starting at Eq. (3.27) and ending at Sec. III B.

[18]A. Pais and R. Serber, Phys. Rev. 113, 955 (1959).

[19]Nevertheless, the parameter space of the Euler angles can be extended to the standard choice, since the redundant regions of integration can be eliminated through proper normalization of the wave functions.

[20]G. Arfken, *Mathematical Methods for Physicists* (Academic, New York, 1970). Chap. 2.

[21]K. Gottfried, *Quantum Mechanics* (Benjamin, New York, 1966), Vol. I.